

Historical Irrigation Water Use and Groundwater Pumpage Estimates in the Harney Basin, Oregon, 1991–2018

By Jordan Beamer, PhD, RG and Mellony Hoskinson

Open File Report No. 2021-02



State of Oregon

Water Resources Department

Salem, Oregon

September 2021



ACKNOWLEDGEMENTS

The authors gratefully acknowledge Ken Stahr and Jonathan La Marche (Oregon Water Resources Department - OWRD) for helpful guidance and reviews; Justin Huntington, Richard Jasoni, and John Volk (Desert Research Institute) for collection, processing, and sharing of eddy covariance ET data; Rachel LovellFord and Harmony Burrigh (OWRD) for coordination with local landowners and water planning efforts; Amanda Garcia (United States Geological Survey - USGS) for supplying datasets and helpful insight and collaboration; Oregon State Representative Mark Owens (landowner) for providing land access for data collection; Karen Moon (Harney County Watershed Council) for collaboration in acquiring and aligning funding, and the Harney Basin Groundwater Study Advisory Committee for providing local hydrologic perspective.

Funding to support this project was provided by NASA Water Resources Applied Sciences Program Grant # NNX17AF53G for providing state water agency staff access to the tools, training, and technical support required to create maps of historical evapotranspiration (ET) from irrigated areas using satellite-based remote sensing models in the Harney Basin and the Oregon Watershed Enhancement Board Monitoring Grant # 219-5046-16766 for funding the ET data collection and partnership with the Harney County Watershed Council.

Contents

ACKNOWLEDGEMENTS.....	2
FIGURES.....	4
TABLES.....	4
ACRONYMS AND ABBREVIATIONS	5
ABSTRACT.....	7
1. INTRODUCTION.....	8
2. PREVIOUS WORK.....	9
3. OBJECTIVES	10
4. STUDY AREA	11
5. APPROACH	13
5.1. Data Assimilation	13
5.1.1. Weather Data Preparation.....	13
5.1.2. Image Preparation and Land Cover.....	14
5.1.3. Measured Evapotranspiration	15
5.2. Estimation of Evapotranspiration and Crop Water Use	18
5.2.1. Agricultural Field Boundary Mapping and Attributes	18
5.2.2. Mapping EvapoTranspiration at High Resolution with Internalized Calibration (METRIC) Model	21
5.3. Estimation of Groundwater Pumpage	29
5.3.1. Validation with Pumpage Datasets.....	29
5.3.2. Water Budget Measurements – Case Example.....	31
5.3.3. Pumpage from Fields Irrigated with Groundwater and Surface Water.....	31
5.3.4. Regional Groundwater Pumpage Estimates	33
6. RESULTS.....	33
6.1. Crop Water Use Rates.....	33
6.2. Crop Water Use Volumes.....	41
6.3. Groundwater Pumpage Volumes.....	43
7. DISCUSSION.....	46
8. REFERENCES	48
APPENDIX A. GLOSSARY OF TERMS	52

FIGURES

Figure 1. Locator map of the major Harney Basin regions.	12
Figure 2. Clear Landsat scenes used in this analysis to process METRIC.	15
Figure 3. Eddy covariance station (CRN) at groundwater irrigated site, Owens Hay Farm, May 2019.	16
Figure 4. Digitized field boundaries in the central GHVA for 1991 and 2016.	19
Figure 5. Mapped irrigated field boundaries in the GHVA for 2016 with water source type identified, where GW right indicates groundwater source type, SW right indicates surface water source type, and GW right on SW right indicates combination source type.	20
Figure 6. Conceptual diagram of datasets and workflow to generate field-level ET estimates using the METRIC model.	25
Figure 7. Scatterplot comparing daily (24-hr) ET at the Alfalfa ET station with METRIC daily ET on the 25 Landsat overpass dates between March 2018 and August 2019.	26
Figure 8. Plot showing daily time series of METRIC interpolated ETrF, CRN station ETrF, with overpass dates and reported field cutting dates for May-September 2018.	28
Figure 9. Plot showing daily time series of METRIC interpolated ETrF, CRN station ETrF, with overpass dates and reported field cutting dates for May-August 2019.	28
Figure 10. Scatterplot of METRIC field-scale seasonal ET volumes (x-axis) and reported seasonal pumpage volumes (y-axis) from 23 pumping well facilities in the Harney Basin for years 2014-2016.	30
Figure 11. Net ET for Harney Basin, May-September 1991.	35
Figure 12. Net ET for Harney Basin and location of ET station, May-September 2018.	36
Figure 13. Irrigated fields by irrigation water source type, Harney Basin, 1991.	37
Figure 14. Irrigated fields by irrigation water source type, Harney Basin, 2018.	38
Figure 15. Annual time series of summed irrigated acres in the Harney Basin for all irrigated fields, except the MNWR, by irrigation water source type.	39
Figure 16. Spatially averaged mean cumulative water year adjusted METRIC ET and gridMET precipitation for years 2014-2018 by irrigation water source type, Harney Basin, Oregon.	41
Figure 17. Time series of annual net evapotranspiration volume from irrigated areas by irrigation source type, Harney Basin, Oregon.	42
Figure 18. Time series of groundwater pumpage in the Harney basin from 1991 to 2018.	44
Figure 19. Mean monthly groundwater pumpage volume for 2014 to 2018 for fields irrigated with groundwater only and combined groundwater and surface water.	44

TABLES

Table 1. Monthly bias correction factors applied to the daily gridMET reference ET (ETr).	14
Table 2. Summary of irrigation systems in the GHVA for 2016 by irrigation source type.	21
Table 3. Mean monthly values for September 2017 to Aug 2019 time period.	27
Table 4. Seasonal total ET for two irrigation seasons at Alfalfa EC station.	27
Table 5. Measured irrigation (IRR), precipitation (PPT), and evapotranspiration (ET) totals from the Harney Alfalfa EC station, years 2018 and 2019.	31

Table 6. METRIC adjusted net ET volume, reported pumpage, and estimated portion of ET from pumped groundwater from field irrigated by well HARN 852 for 2014-2016 at EOARC.....	32
Table 7. May through September Net Evapotranspiration Rates, in feet, by irrigation source type	40
Table 8. Mean seasonal May through September net evapotranspiration and pumpage rates by irrigation source and region, 1991-2018, Harney Basin, Oregon.	40
Table 9. May to September Net ET Volumes, in acre-feet x 1000, by irrigation source type	43
Table 10. Total estimated seasonal groundwater pumpage from agricultural irrigation wells, Harney Basin, Oregon.....	45
Table 11. Total estimated groundwater pumpage by major drainage basin in GHVA, for select years between 1991 and 2018 and averaged for 5-year period 2014 to 2018.....	46

ACRONYMS AND ABBREVIATIONS

AFY	acre-feet per year
ASCE	American Society of Civil Engineers
BR	Bowen ratio
CIMIC	Calibration using Inverse Modeling at Extreme Conditions
CLU	Common Land Unit
CU	consumptive use
CDL	Cropland Data Layer
DEM	Digital Elevation Model
EBR	energy-balance ratio
EC	Eddy Covariance
EOARC	Eastern Oregon Agricultural Research Station
EROS	Earth Resources Observation and Science
ET	evapotranspiration
ETa	actual evapotranspiration
ETc	corrected evapotranspiration
ETnet	net evapotranspiration
ETM+	Enhanced Thematic Mapper Plus
ETo	grass-reference evapotranspiration
ETr	alfalfa-reference evapotranspiration
ETrF	fraction of reference ET, computed as $ETrF = ET / ETr$
FGDC	Federal Geographic Data Committee
FMASK	Function of Mask
G	soil heat flux
GHVA	Greater Harney Valley Area
GridMET	gridded meteorological data
GW	groundwater
H	sensible heat flux
IRR	irrigation

Kc	crop coefficient
LE	latent heat flux
LEPA	low-energy precision application
LESA	low-elevation sprinkler application
MESA	mid-elevation sprinkler application
METRIC	Mapping Evapotranspiration using high Resolution and Internalized Calibration
MNWR	Malheur National Wildlife Refuge
NAIP	National Agriculture Imagery Program
NDVI	normalized difference vegetation index
NIWR	net irrigation water requirement
NLDAS	North American Land Data Assimilation System
OLI	Operational Land Imager
OWRD	Oregon Water Resources Department
PLSS	Public Land Survey System
POU	OWRD water rights Place of Use GIS Layer
PPT	total precipitation
PRISM	Parameter-elevation Regressions on Independent Slopes Model
QAQC	Quality Assurance and Quality Control
Rn	net radiation
r ²	coefficient of determination
SEB	surface energy balance
SSURGO	Soil Survey Geographic Database
SW	surface water
TM	Thematic Mapper
TOA	top of atmosphere
USDA	United States Department of Agriculture
USGS	U.S. Geological Survey
USFWS	U.S. Fish and Wildlife Service
VWC	volumetric water content
WBAL	water balance
WRS2	Worldwide Reference System-2
WSWUP	Western States Water Use Program
WY	water year

ABSTRACT

Current and historical crop water use and groundwater pumpage estimates are needed for the Harney Basin in southeastern Oregon for a complete evaluation of the basin's groundwater budget. This will inform the overarching cooperative Oregon Water Resources Department (OWRD) and U.S. Geological Survey (USGS) study of the groundwater resource. This open file report describes the process used by OWRD to quantify crop water use from agricultural fields and associated groundwater pumpage in the Greater Harney Valley Area (GHVA) and presents findings of the analysis. Evapotranspiration (ET), consumptive use (CU; ET minus precipitation), and groundwater pumpage were estimated for 13 individual years spanning 1991 to 2018. The average annual growing season for irrigated areas was assumed to occur from May to September.

ET of applied surface water and groundwater and groundwater pumpage for irrigation during 1991-2018 were estimated by coupling modeled field level ET estimates with available groundwater-pumpage data. Field-level ET was estimated using a remotely-sensed ET model - Mapping EvapoTranspiration at High Resolution with Internalized Calibration (METRIC) - scaled to ET measurements from an alfalfa field in the basin, GridMET precipitation data, and mapped agricultural fields. The source of water used to irrigate each field was obtained from OWRD water rights information. Estimated pumpage volumes associated with each ET estimates were determined using reported pumpage volumes from OWRD's Water Use Reporting database and literature-reported irrigation efficiencies. The METRIC estimated average growing season net ET (ET minus precipitation) for mapped irrigated fields over 1991 to 2018 was 1.51 feet per year (ft/yr) for fields irrigated with primarily groundwater, 1.49 ft/yr for fields irrigated with combined groundwater and surface water, and 1.43 ft/yr for fields irrigated with primarily surface water.

In order to facilitate comparison of recharge and discharge volumes and evaluate groundwater development in the USGS groundwater study, the Harney Basin was separated into three analysis regions based on topography and groundwater movement. Current groundwater pumpage estimates for each region represent the mean-annual values of pumpage for the five year period of 2014 to 2018. The mean annual groundwater pumpage volume for each region is as follows: 76,000 acre-feet for the northern region, 20,000 acre-feet in the southern region, and 41,000 acre-feet in western region. The average total pumpage estimate for the GHVA area during 2014-2018 is estimated at 140,000 acre-feet per year from 67,400 groundwater irrigated acres, which represents an increase of 80,000-90,000 acre-feet since the early 1990s. Regional groundwater pumpage rates for fields irrigated with primary groundwater rights averaged 2.16 acre-feet per acre (ac-ft/ac), whereas rates for fields irrigated with supplementary groundwater rights averaged 1.24 ac-ft/ac.

1. INTRODUCTION

Agricultural communities in the arid high desert of eastern Oregon rely heavily on water supplied by surface water diversions and pumped groundwater. Accurate reporting of irrigation water use is needed by OWRD and USGS to support surface and groundwater use studies, develop historical groundwater pumpage estimates, and for basin water planning and management.

Like many places in the intermountain west, water use in southeastern Oregon is dominated by irrigated agriculture. Surface water availability for irrigation largely depends on precipitation (PPT) in the form of snow. Surface water has been fully allocated for decades, beginning in the 1960s, and for years with low-to-average snowpack, there is little surface water available during the irrigation season (Cooper, 2002). In years with insufficient snowpack to meet surface water allocations, supplemental groundwater is used. Because surface water is generally fully allocated, new irrigation water demand since about the 1970s has relied on groundwater sources, and has led to increasing pumpage and declining groundwater levels over time.

In the Harney Basin, groundwater supports the needs of rural communities, ecosystems, and the local economy. Starting in the early 2000s, OWRD began to observe declining groundwater levels in several areas throughout the basin. A preliminary estimate of groundwater use in 2015 indicated that the volume of permitted groundwater use likely exceeded the estimated annual net recharge (Grondin, 2015). In 2015, the permitted acreage for groundwater irrigation in the Harney basin was 95,700 acres (Grondin, 2015). Applying a standard duty of 3 acre-feet per acre for groundwater irrigation in the Harney Basin, total groundwater allocations amount to 287,000 acre-feet per year. In comparison, the estimated annual recharge for the entire Harney Basin is 260,000 acre-feet per year (Robison, 1968). The total annual groundwater allocations for irrigation in the GHVA alone exceeds the groundwater budget of the entire basin, indicating that the groundwater resource is over appropriated [OAR 690-400-0010-(11)(a)(b)].

Following widespread concern throughout the basin about sustainability of the groundwater resource and future groundwater development, in 2016 OWRD established a Groundwater Area of Concern in the Greater Harney Valley Area (GHVA) and stopped issuing new groundwater permits within the GHVA pending completion of a comprehensive groundwater study. In 2016, OWRD entered into a cooperative agreement with the U.S. Geological Survey (USGS) to conduct a groundwater availability study of the Harney Basin (Garcia and others, 2021; Gingerich and others, 2021).

In order to effectively manage groundwater in the basin and as part of the Harney Basin groundwater study, development of an accurate groundwater budget is required. The budget is based on estimates of how much water enters the basin (groundwater recharge or inflow), how much exits the basin (groundwater discharge or outflow), and how much aquifer storage is changing in the basin. The Harney Basin is a predominantly closed, internally drained basin with no surface water outflow. Evapotranspiration (ET) from groundwater irrigation and phreatophytes represent the greatest sources of anthropogenic and natural groundwater discharge, respectively (Garcia and others, 2021). ET is the combination of evaporation from soil and plant surfaces and transpiration of the plant, and is the primary determinant of crop consumptive use (CU) rates. Within the Great Basin, and other regions

where groundwater discharge is primarily due to ET, groundwater discharge is considered the most reliable groundwater budget component (Bredehoeft, 2007).

Direct estimates of historical water use for irrigation, such as metered pumpage data from groundwater wells and gaged diversions from surface water sources, are scarce or non-existent and thus need to be estimated indirectly. Previous estimates of historical groundwater pumpage for irrigation in Oregon have typically been computed as the product of historical irrigated acreage and assumed crop consumptive use (ET) rates that are constant in space and time and assume optimum crop irrigation and health, divided by an assumed irrigation-system efficiency value (Conlon and others, 2005; Gannett and others, 2001; Gannett and others, 2007). However, crop consumptive use rates (as well as irrigated acres and system efficiency) vary in space and time due to factors such as water availability, crop type, crop health and phenology, growing season length, irrigation management, and weather conditions (i.e. solar radiation, air temperature, relative humidity, and wind speed). Satellite-based remote sensing that has been verified with ground-based measurements provides a mechanism to observe field conditions and changes in ET caused by these factors over large areas and time periods, and thus has been shown in previous studies to be useful for water resources management. Satellite imagery captures field conditions and spatial and temporal variability in crop phenology, stress, management, and ultimately ET and water use (Anderson and others, 2012).

Where available, field-scale crop water use estimates reasonably compare with measured groundwater pumpage data. Therefore, relationships between crop water use and measured groundwater pumpage can be used to extrapolate pumpage estimates across a basin for time periods and fields where records do not exist. This study uses Landsat satellite imagery and the METRIC ET model to estimate field-scale ET and groundwater pumpage volumes. In addition, this study illustrates the utility of satellite-based ET as a cost-effective approach for estimating historical groundwater pumping at the basin-scale over long time periods of time. The approach is more accurate than using historical potential crop coefficients (K_c), reference ET (ET_{ref}), and irrigated area approaches.

2. PREVIOUS WORK

The 1992 report *Oregon Crop Water Use and Irrigation Requirements* by Cuenca et al. (1992) provides estimates of monthly and growing season crop ET and net irrigation water requirements (NIWR) for 27 different agricultural regions in Oregon, including hydrologic basins in southeast Oregon. Cuenca et al. (1992) applied the FAO-24 Blaney-Criddle method (Doorenbos and Pruitt, 1977) to estimate grass reference ET (ET_o) on a monthly basis and effective precipitation using weather data summarized from 244 National Weather Service stations (including Harney Basin). Crop ET is estimated by multiplying the ET_o by a grass-related K_c . The Blaney-Criddle approach to estimate crop ET assumes well-watered and stress-free conditions throughout a pre-defined irrigation season (potential crop ET), and has been applied across Oregon for irrigation planning and design. The Cuenca et al. (1992) estimates represent the potential crop ET based on ET_o rather than the actual crop ET that occurs as a result of spatial and temporal variations in water availability, crop stress and disease, crop management, irrigation and land management, and climatic conditions. The use of this method has since been superseded by the American Society of Civil Engineers (ASCE) standardized Penman-Monteith equation (ASCE, 2005).

The West-Wide Climate Risk Assessment: Irrigation Demand and Reservoir Evaporation Projections (WWCRA) study (Huntington, J. L. and others, 2015) applied the U.S Bureau of Reclamation (BOR) ET Demands model to seven major river basins in the western United States including the Columbia and Klamath basins in Oregon. The ET Demands model uses the ASCE standardized Penman-Monteith reference ET equation for a short grass reference (ET_o) and the dual Kc-ET_o method (Allen and others, 1998). Similar to the Cuenca approach, this method estimates potential ET for irrigated crops which is valuable for establishing the upper bound of crop ET, but will overestimate actual ET under water short conditions or other non-ideal conditions that cause plant stress.

The satellite-based METRIC model has been applied to estimate field-scale crop ET in the Klamath Basin of south central Oregon (Cuenca et al., 2013; Zhao et al., 2015) and in the Powder River Basin of Eastern Oregon (Zhao, W. and others, 2014; Zhao, W. and others, 2015). METRIC ET estimates in Klamath (2010) were about 9 percent above eddy-covariance ET estimates on average at two native vegetation wetland (bulrush and marsh) sites (J. Haynes, written commun. 2021). Cuenca et al. (2013) compared seasonal (May-September) ET estimates from METRIC in the Wood River Valley (Klamath Basin) with in-situ estimates of seasonal ET derived from two Bowen ratio (BR) energy balance stations located in unirrigated and irrigated pasture grass. METRIC seasonal ET estimates agreed well with measurements at the unirrigated and irrigated BR stations, with differences of 2.6 percent and 2.3 percent, respectively.

3. OBJECTIVES

The main objectives of this study are to estimate historical and current irrigated acreage, field- and regional-scale crop irrigation water use, and groundwater pumpage for irrigation within the GHVA. The four primary tasks to achieve the objectives include:

- Develop and report field-scale estimates of ET for irrigated fields within the Greater Harney Valley Area (GHVA) of southeastern Oregon using Landsat satellite imagery and a satellite-based ET model for the irrigation season (May 1 to September 30) during the period 1991 to 2018
- Adjust satellite-based ET estimates using in-situ estimates of ET made from eddy covariance stations from September 2017 to August 2019
- Correlate field-scale satellite-based ET with groundwater pumpage estimates to develop a locally derived relationship between ET and pumpage to estimate historical groundwater pumpage basin-wide
- Assess and summarize field-scale seasonal and monthly ET estimates for all irrigated fields in the Harney Basin, and partition field-scale estimates and summarize results by areas irrigated with groundwater only, surface water only, and a combination of groundwater and surface water

The results from this study provide current and historical irrigation water use, groundwater pumpage and irrigated acreage estimates required for the Harney Basin of southeastern Oregon to inform the basin's water budget analysis for the cooperative Oregon Water Resource Department (OWRD) and U.S. Geological Survey (USGS) groundwater basin study, and local water planning efforts.

4. STUDY AREA

The Harney Basin encompasses about 5,240 square miles in southeastern Oregon. Irrigation from pumped groundwater predominantly occurs in the GHVA, which lies within central Harney Basin (Figure 1) and was used as the study area in this report. Hydrologically, three major watersheds comprise the GHVA. The State of Oregon (State of Oregon Water Resources Board, 1967) identify these watersheds as Silver Creek (Western Region), Silvies River (Northern Region), and Donner und Blitzen River (Southern Region). The elevation of the agricultural area within the GHVA ranges from 4,100 feet near Malheur Lake to 4,300 feet in Silver Creek Valley. The GHVA climate is characterized as semi-arid with long, cold winters, and short, mild summers, a wide range of daily and seasonal temperatures, and precipitation mostly occurring from November to June (Oregon State Water Resources Board, 1967). Mean annual precipitation from 1981 to 2010 ranged from 9 to 12 inches within the agricultural areas on the valley floor, with approximately 80 percent of precipitation occurring during winter months and growing season total precipitation averaging about 2.5 inches (Oregon State University PRISM Climate Group). The hottest month is July with an average high of 85 °F, and the coldest month is January, with an average low of 16 °F (Oregon State University PRISM Climate Group).

Irrigated alfalfa and grass hay are the principal crops grown within the study area, with marginal amounts of spring and winter grains, and mint (USDA National Agricultural Statistics Service, 2018). The typical growing season is May to September. Alfalfa and grass hay crops are typically harvested (i.e. cut and baled) from 3 to 4, and 1 to 2 times per year, respectively. Agricultural fields irrigated with pumped groundwater only are predominantly irrigated with a primary groundwater right, and fields irrigated with a combination of both groundwater and surface water are irrigated with a primary surface water right and a supplementary groundwater right. A primary water right means the water right designated by OWRD as the principle water supply for the authorized use. A supplemental water right means an additional appropriation of water to make up a deficiency in supply from an existing water right, used in conjunction with a primary water right.

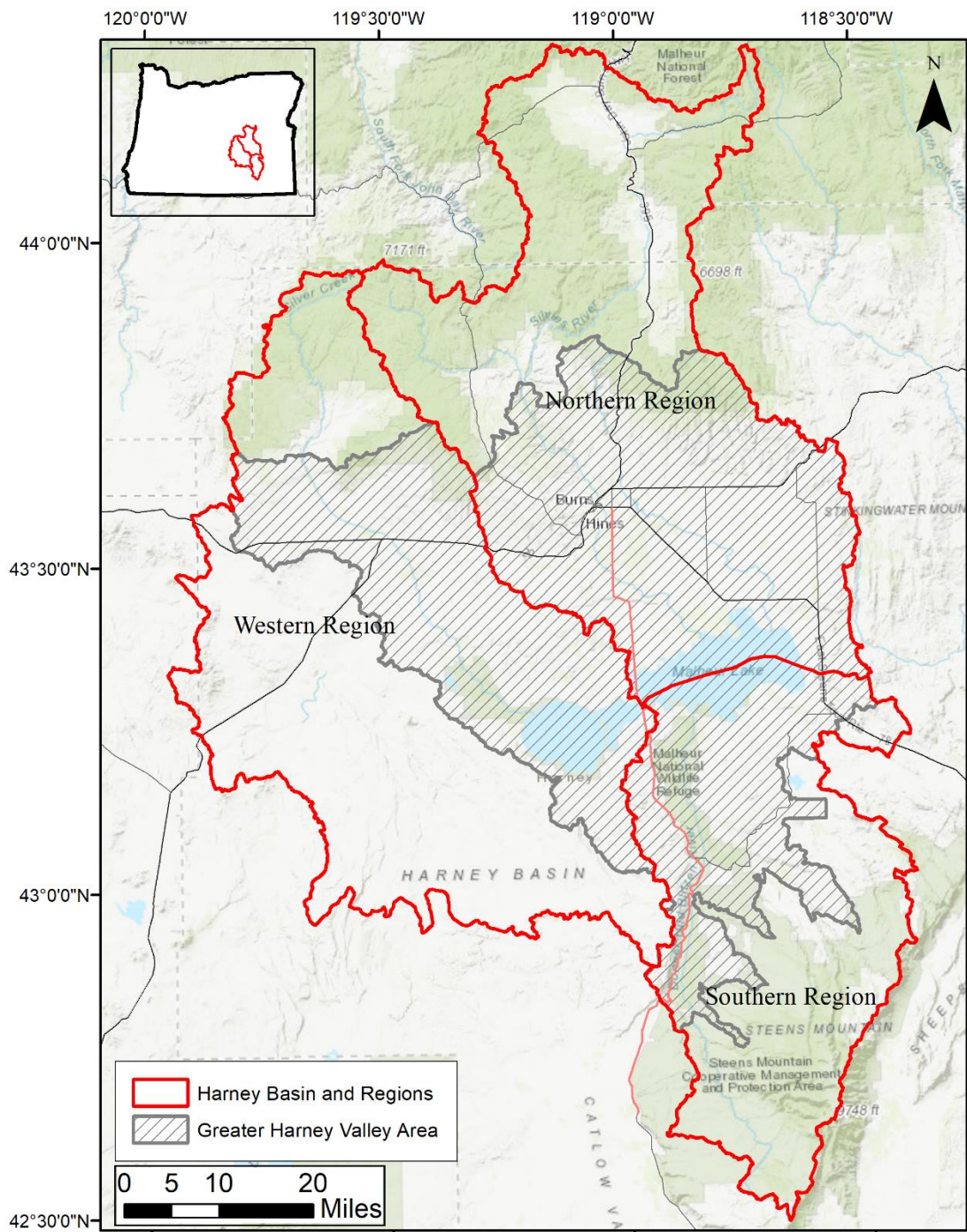


Figure 1. Locator map of the major Harney Basin regions.

5. APPROACH

The general approach to accomplish the objectives of this project were to 1) apply a satellite-based ET model to estimate the spatial distribution of actual ET at the field scale from calendar year 1991 to 2018, and 2) summarize field-scale total ET and net ET (total ET less PPT) for specific time periods and areas of interest. The primary datasets used for estimating historical crop water use and groundwater pumpage include:

- Landsat data from a single path-row covering the GHVA study area (path 43, row 30),
- field-scale, monthly ET,
- field-scale, monthly PPT,
- reference ET,
- mapped irrigated field boundaries,
- water rights information,
- in-situ ET estimates, and
- user-reported groundwater pumpage data estimates using primarily flowmeters

5.1. Data Assimilation

5.1.1. Weather Data Preparation

The METRIC approach used in this study utilizes meteorological data from two gridded weather products, the ASCE Penman-Monteith alfalfa reference ET (ET_r) from the North American Land Data Assimilation System (NLDAS) (Cosgrove and others, 2003) available at an hourly time step and 12-km grid (391 grid cells in the Landsat scene), and ET_r and precipitation products from the Gridded Surface Meteorological Dataset (gridMET) (Abatzoglou, 2013) available on a daily time step and 4-km grid (3,196 grid cells in the Landsat scene). Both datasets are available for the study area and analysis period (1991–2018). The NLDAS ET_r data was used as input into METRIC to estimate the “instantaneous” reference ET rate at the time of satellite overpass. The gridMET ET_r was used as input into METRIC to perform time integration, and estimate daily, monthly, and annual actual ET (further described below). Precipitation data from gridMET were used to estimate annual and monthly precipitation totals, and compute net ET (ET minus precipitation) from agricultural areas.

A comparison of gridMET ET_r with ET_r computed using in-situ weather data was used to account for potential bias in the gridded product. Long-term historical in-situ weather data representative of agricultural conditions in the GHVA was not available for the historical analysis. Therefore, this assessment was accomplished by comparing gridMET ET_r to ET_r computed at 19 of the nearest U. S. Bureau of Reclamation Pacific Northwest AgriMet stations collecting weather data representative of agricultural weather conditions in Oregon, Idaho, and California (<https://www.usbr.gov/pn/agrimet/agrimetmap/agrimap.html>; last accessed July 24, 2018). The period of overlap between the available daily AgriMet ET_r and gridMET ET_r data was the 15-year period between 2003 and 2017. Similar to what (Abatzoglou, 2013) found at southern Idaho AgriMet stations, gridMET ET_r was consistently 10-15 percent higher than AgriMet ET_r during the growing season months. Cooler, wetter environments surrounding agricultural areas commonly lead to reduced ET_r with respect to warmer and drier natural areas. The observed bias in gridMET ET_r with respect to AgriMet ET_r is likely

because weather stations used to inform gridMET are often located in airports or ambient areas characteristic of the natural landscape rather than agricultural areas. In order to bias-correct the gridMET ETr, mean monthly ratios of AgriMet ETr to gridMET ETr (ratio = AgriMet ETr / gridMET ETr) were computed at each of the 19 nearest AgriMet stations and then interpolated using inverse distance weighting, and then spatially averaged to agricultural fields in the basin (Table 1). Results indicate that on average the annual ratio was 87 percent. As an additional validation step, a comparison was made between monthly ETr totals computed at the irrigated alfalfa eddy-covariance (EC) station, CRN, with gridMET ETr for the grid cell overlying the station location. For the period September 2017-August 2019 the average annual ratio of 89 percent was computed at the station, similar to that computed using AgriMet stations.

Table 1. Monthly bias correction factors applied to the daily gridMET reference ET (ETr).

Month	Jan	Feb	Mar	Apr	May	Jun	Jul	Aug	Sep	Oct	Nov	Dec	Ann
Ratio	0.80	0.87	0.90	0.93	0.91	0.91	0.90	0.87	0.86	0.82	0.81	0.83	0.87

5.1.2. Image Preparation and Land Cover

Reflectance and thermal imagery from Landsat 5, Landsat 7, and Landsat 8 were used to compute METRIC ET over 14 individual years from calendar year 1991-2019. The pixel size for Landsat data is 30 m x 30 m. This spatial resolution allows for accurate quantification of ET at the field-scale. The GHVA study area is within a single Landsat scene, path 43, row 30.

The METRIC model requires clear Landsat scenes in order to accurately estimate ET, therefore scenes during the full Landsat record (1984 to 2019) were evaluated to select the years with the most cloud-free scenes during the agricultural growing season (May–September). An open-source tool called Clear Scene Counter for Landsat (<https://github.com/WSWUP/cloud-free-scene-counts>) was used to gather image files of all available Landsat scenes. For each year, Landsat images with excessive cloudy, smoky, snowy, or otherwise unsuitable conditions on the GHVA were manually discarded. The year 1991 was selected as the beginning year of analysis to observe the increase in groundwater irrigation that began in the early 1990s. The years from 1991 through 2019 with the most cloud-free growing-season scenes were compared with years where high-resolution National Aerial Imagery Program (NAIP) (USDA, 2016) imagery was available which was necessary for the field boundary mapping task. In addition, these years were evaluated to ensure that they characterized a range of wet-to-dry conditions for assessing how surface water and groundwater use changes during wet and dry years. The years selected for analysis include: 1991, 1992, 1994, 2000, 2001, 2005, 2009, 2011, and 2014 to 19.

For the selected “clear” scenes that had minimal cloud cover but were usable, the FMask (Function of Mask) cloud mask was used to automatically mask clouds, cloud shadows, and snow from the Landsat images (Foga and others, 2017). The number of Landsat scenes used per year ranged from 10 scenes in 1991 (Landsat 5 only) to 28 scenes in 2016 (Landsat 7 and 8). For some years, cloud-free Landsat scenes were not available for every month, so the analyses reported here are most accurate for cloud-free time periods and may not represent the ET patterns for the entire year. The majority of years analyzed had at

least one scene available per month during the growing season, generally May-September (approx. day of year 120 to 270 as shown in Figure 2) to adequately observe crop phenology and management.

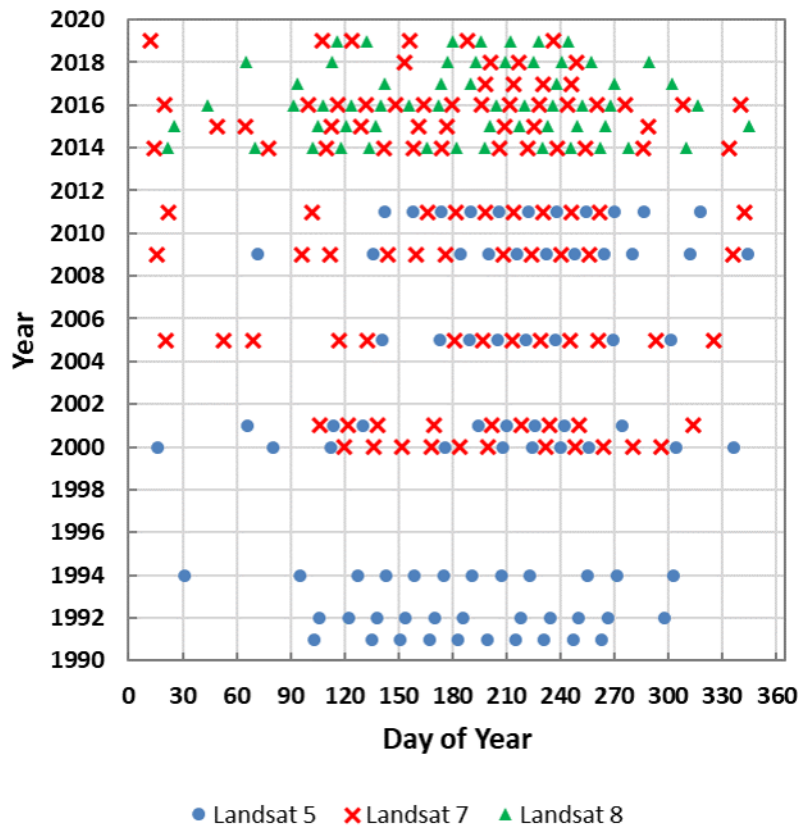


Figure 2. Clear Landsat scenes used in this analysis to process METRIC.

5.1.3. Measured Evapotranspiration

Modeled ET estimates have been validated over multiple eddy covariance (EC) and Bowen ratio (BR) flux stations in past studies. Morton et al. (2013) compared METRIC ET with measured ET from 8 EC and BR stations located in western Nevada. Using a fetch area of 100-m radius around the stations to summarize METRIC ET, the mean daily ET for each Landsat overpass date had an r^2 of 0.80 with standard error of 0.98 mm, and the growing season mean daily ET compared from April 1 to October 31 (mean daily ET = 4.2 mm) had an r^2 of 0.70 with standard error of 0.50 mm.

In this study, METRIC ET was adjusted to match ET measurements from an EC station – CRN - located in a representative groundwater-irrigated alfalfa field near Crane, Oregon (Figure 3). The ET measurements were collected and processed by the Desert Research Institute (R. Jasoni, 2019, written communication). The EC station is located in the center of a 120-acre center pivot alfalfa field (43.417149°, -118.604263°) that is irrigated from late April /early May to mid-September and harvested 3 to 4 times per growing season.



Figure 3. Eddy covariance station (CRN) at groundwater irrigated site, Owens Hay Farm, May 2019.

The EC flux data from the CRN station was processed using widely accepted methods as outlined in (Arnone and others, 2008) and corrected for energy balance closure using the energy balance ratio method (Foken, 2008; Twine and others, 2000) to compute daily and monthly ET summaries from September 2017 to August 2019. Gap filling procedures to fill in missing daily ET data based on the gridMET ETr data were also applied using a procedure like that in the FLUXNET2015 processing pipeline (Pastorello and others, 2020). The fluxes were post-processed and corrected to create daily and monthly time series using the flux-data-qaqc Python program (Volk and others, review pending). The average energy balance ratio (ratio of turbulent fluxes to available energy) of the daily time series from raw latent (LE) data was about 0.8 (i.e. turbulent fluxes were 80 percent of available energy).

METRIC ET and measured ET were compared at daily, monthly, and seasonal time scales. Validation was performed by comparing measured ET with METRIC ET estimates averaged for a circular footprint with a radius of 650-ft (200-m) surrounding the EC station location, assumed to represent the ET measurement area.

5.1.3.1. Eddy covariance method

The EC method is based on the determination of the turbulent fluxes of latent and sensible heat (Brutsaert, 1982). Each of the energy components are calculated independently, unlike the Bowen ratio method. EC stations are equipped with a sonic anemometer, gas analyzer, and thermocouple to measure changes in vertical wind speed, vapor density, and temperature, respectively (Fig. 3). Sensible heat flux (H) is calculated using the equation:

$$H = \rho_a \cdot c_p \cdot \overline{w' \cdot \theta'} \quad (1)$$

Where

H	= the sensible heat flux (energy per area)
ρ_a	= is density of the air (mass per volume)
w'	= the turbulent vertical wind velocity
θ'	= the deviation in temperature
c_p	= the specific heat capacity

ET is computed as the covariance of the vertical wind speed (w') and humidity (q'). The formula for computing evapotranspiration is:

$$ET = \rho_a \cdot \overline{w' \cdot q'} \quad (2)$$

Where

ET	= the evapotranspiration rate (length per unit time)
ρ_a	= is density of the air (mass per volume)
w'	= the turbulent vertical wind velocity
q'	= the deviation in humidity

The advantage of the EC method is the direct measurement of both ET and H independently. In addition, this approach can be more accurate compared to other energy budget methods (i.e. BR) because ET and H are not forced to balance. However, independent measurements of ET and H rarely achieve full energy budget closure. Meyers and Baldocchi (2005) suggested that the mean uncertainty for ET measurement from a perfectly designed and maintained EC system can approach 10 percent.

5.1.3.2. Site instrumentation installation, EC calculation, and data QA/QC

The single EC station at the groundwater irrigated alfalfa site near Crane was installed in September 2017. Instrumentation installed at the EC station consists of a three-dimensional sonic anemometer (CSAT3, Campbell Scientific Inc., Logan, Utah, USA) installed at a height of 2.0 m to measure the three wind components, and an open-path infrared gas analyzer (IRGA; LI-7500, LI-COR Inc., Lincoln, Nebraska, USA) installed at a height of 2.0 m to measure H_2O molar density. Weather and soil instruments at the site consists of a shielded air temperature and humidity sensor at a height of 2.6 m (HMP 45C; Vaisala, Helsinki, Finland), a wind vane anemometer at a height of 2.6 m (3001 Wind Sentry; R.M. Young Company, Traverse City, MI, USA), a net radiometer at a height of 2.1 m (CNR4; Kipp and Zonen, The Netherlands), a photosynthetically active radiation (PAR, 400-700 nm) sensor at a height of 2.5 m (LI-910; LI-COR Inc., Lincoln NE, USA), a tipping bucket rain gauge at a height of 2.5 m (TE525MM; Texas Electronics, Dallas TX, USA), soil heat flux plates at a depth of 8 cm (HFP01SC; Hukseflux, The Netherlands) (four at each site), averaging soil temperature thermocouple probes (TCAV; Campbell Scientific, Logan, UT, USA) (two pair at each site) at depths of 2 and 6 cm (gives on average temperature), and volumetric soil moisture probes (CS616; Campbell Scientific, Logan, UT, USA) (two at each site) at a depth of 2.5 cm. An Apogee bulk precipitation gauge was installed at the site. Data from all instruments were recorded with a data logger (CR5000, Campbell Scientific) at a frequency of 10 Hz (10 times per second).

Average ET for each half-hour period, including H and LE heat fluxes, was measured using the EC method (Baldocchi and others, 2001; Baldocchi, 2003). Raw data (10 Hz) of the three wind components, the speed of sound, and H₂O molar density were post-processed using EdiRe software (University of Edinburgh, 2013). LE was calculated as the covariance between turbulent fluctuations of the vertical wind speed and water vapor density derived from Reynolds (block) averaging using 30-min blocks of data (Arnone and others, 2008). Half-hourly flux data calculated by EdiRe were then quality controlled using a four-step filtering procedure described in (Wohlfahrt and others, 2008).

5.2. Estimation of Evapotranspiration and Crop Water Use

Field-scale monthly ET was summarized by averaging METRIC ET rasters to agricultural field boundaries based on the U.S. Department of Agriculture's (USDA) common land unit (CLU) polygons. CLU field boundaries were manually edited for each study year to reflect changes in agricultural land use over time.

5.2.1. Agricultural Field Boundary Mapping and Attributes

The maximum extent of irrigated areas was delineated within a Geographic Information System (GIS) for all actively irrigated agricultural fields in the GHVA. This was completed for each of the 13 years the METRIC model was run for the Harney basin ranging from 1991 to 2018. Irrigated areas within the Malheur National Wildlife Refuge (MNWR) were based on delineated Habitat Units identified as 'irrigated' and supplied by the U.S. Fish and Wildlife Service (Daniel Craver, written commun., 2017). Irrigated areas in the MNWR were assumed to remain static and were not updated for each year.

5.2.1.1. Digitizing Field Boundaries of Actively Irrigated Fields

Agricultural field boundary polygons were initially obtained from the CLU dataset for Harney County, which were digitized from 2008 digital orthophotos (USDA, 2008). In order to create year specific polygons of actively irrigated fields for each year METRIC was run, the CLU dataset was overlaid on high-resolution aerial imagery from NAIP and OWRD mapped water rights Places of Use (POU) to edit CLU polygons by removing fields that were not cultivated or irrigated, and digitizing (adding) fields missing from CLU dataset. Examples of mapped field boundaries in the central GHVA for 1991 and 2016 are shown in Figure 4. For years without available NAIP imagery, Landsat May-September maximum Normalized Difference Vegetation Index (NDVI) maps available from the Climate Engine cloud computing web application were obtained (Huntington et al., 2017; <http://climateengine.org/>). Using an NDVI threshold of greater than or equal to 0.4, field boundaries were modified as needed to create a complete dataset of actively irrigated polygons in the study area. For each year, individual field boundary polygons were assigned a unique ID and start year of active irrigation (i.e. year when the field was first identified in the imagery as actively irrigated).

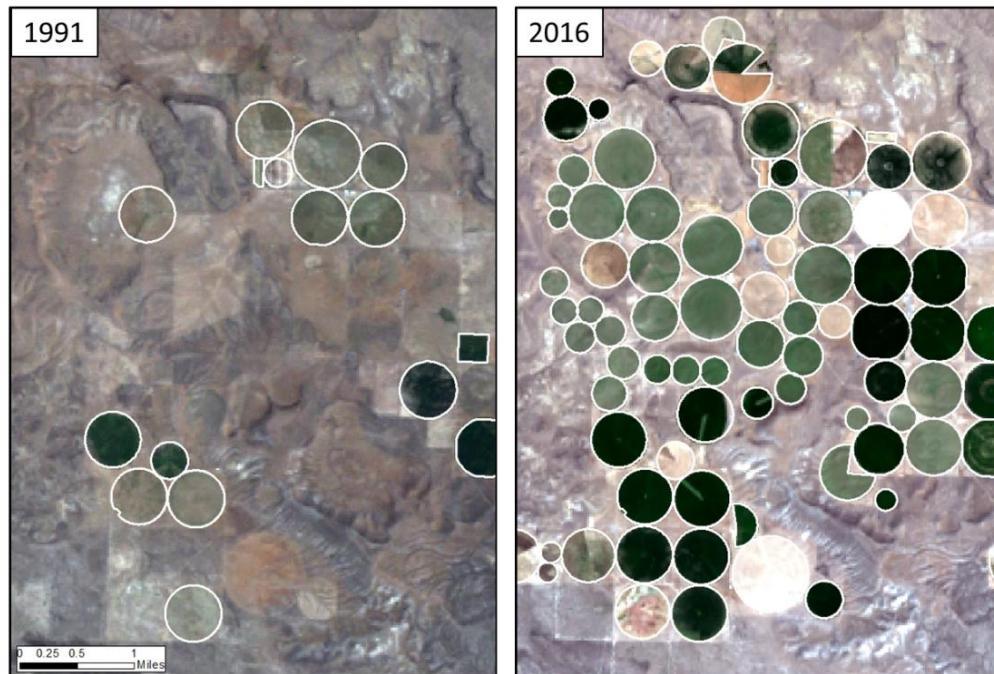


Figure 4. Digitized field boundaries in the central GHVA for 1991 and 2016.

5.2.1.2. Attributing Water Source Type with Mapped Water Rights Place of Use

Yearly field boundary datasets were attributed with one of the following irrigation source types: groundwater irrigated (GW), surface water irrigated (SW), or a combination of groundwater and surface water (GW&SW). The first step in identifying irrigation source type was to overlay yearly field boundaries with the OWRD mapped water rights place of use (POU) dataset. The irrigated POU dataset for the Harney basin were distinguished as having only groundwater rights, only surface water rights, and both surface water and groundwater where they overlapped. For each year METRIC was run, only the POU polygons with priority dates for that year and all years prior were included in the analysis in order to accurately represent irrigation development. Selected POU polygons were then converted to a 30 m raster based on the 30 m USGS National Elevation Dataset (NED) and cells were classified based on the irrigation source type as integer values (1 =GW irrigated, 2 = SW irrigated, 3 = Combination) to create the POU irrigation raster. The POU irrigation raster was then paired with the respective field polygon dataset for the year of interest (for example, year 2000 field polygons paired with the 2000 POU raster characterizing with water rights with priority dates earlier than 1/1/2001). Where the two datasets intersected, the field polygon was assigned the same water source as the majority of the POU pixels. This approach worked for assigning water source type for about 90 percent of the digitized field polygons, and the rest of the fields were manually attributed as described below. It was assumed that all irrigated habitat units within the refuge were irrigated with surface water, with the exception of about 9,000 acres irrigated with spring discharge west of Harney Lake.

5.2.1.3. Identifying Water Source Type for Fields with No Mapped Water Rights Place of Use

Where digitized fields did not overlay a mapped POU, the field location using the Public Land Survey System, or PLSS, was entered into the OWRD Water Rights Information System (<https://apps.wrd.state.or.us/apps/wr/wrinfo/>) to check if a water right existed in the quarter-quarter section, which is the smallest spatial unit (40 acres) in the PLSS. If the quarter-quarter contained water rights but no mapped POU, water rights information was used to assign a water source type to the field. If the field existed in an area with no mapped POU or water right in the section, field staff was contacted and local knowledge and assumptions of source type were made (for example, center pivots generally are groundwater and wheel line and flood generally are SW) and used to assign source type to the small number (~35) of remaining fields. Local OWRD field staff also were contacted to determine if other water right or source-type information was available. The results of the field mapping and water source type classification for 2016 are shown in Figure 5.

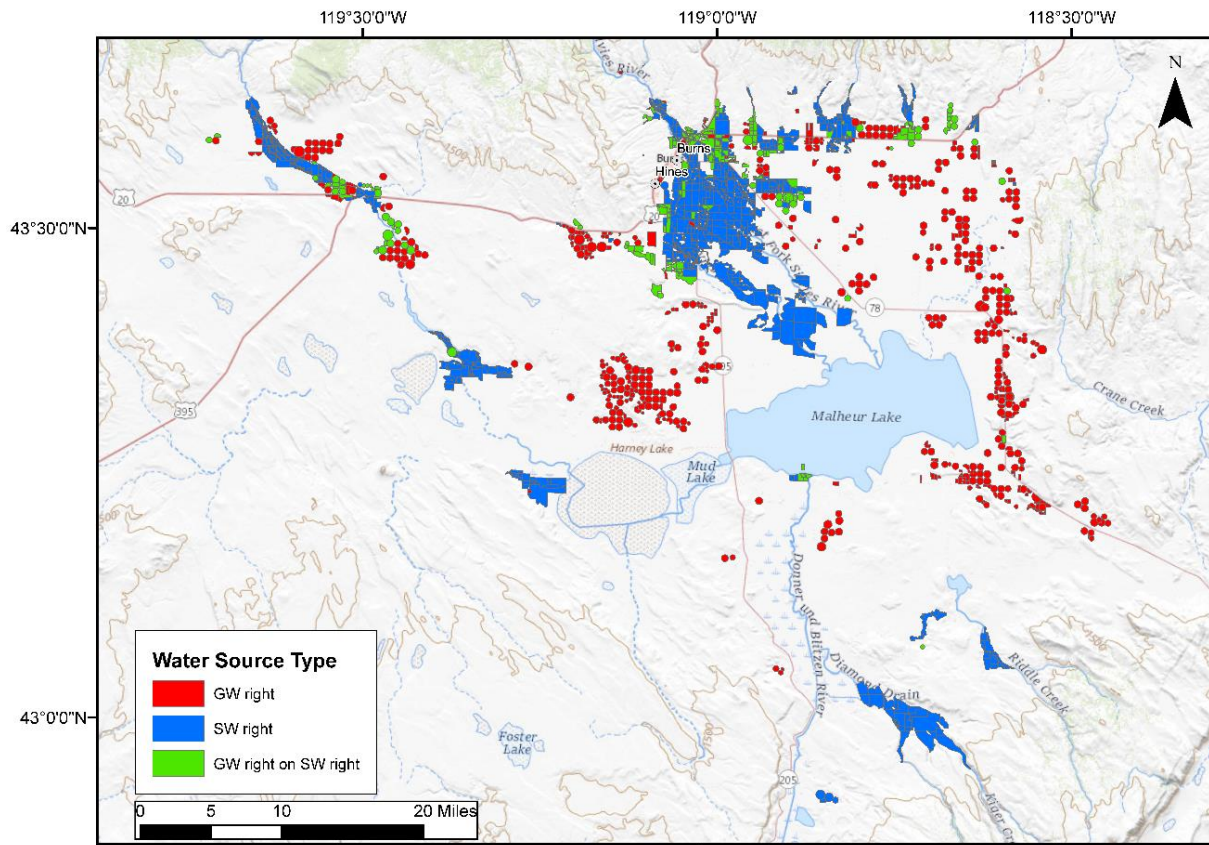


Figure 5. Mapped irrigated field boundaries in the GHVA for 2016 with water source type identified, where GW right indicates groundwater source type, SW right indicates surface water source type, and GW right on SW right indicates combination source type.

5.2.1.4. Identify Irrigation System for each Mapped Field

Information about irrigation systems and irrigation efficiency is needed to estimate pumpage volumes from water use estimates from ET for each groundwater irrigated field. A geospatial assessment was done by overlaying the 2016 mapped field boundaries and NAIP aerial imagery, and visually classifying

the fields using visible equipment and sprinkler patterns into three categories: surface flood, sprinklers (wheel line/handline), and center pivots (Table 2). For 2016 fields, groundwater irrigated fields were dominated by center pivot irrigation, and surface water irrigated fields were dominated by flood irrigation. Fields irrigated with both a combination of surface water and groundwater (green fields in Figure 5) were largely a mixture of surface flooding and center pivots, with a smaller amount of sprinkler systems.

Table 2. Summary of irrigation systems in the GHVA for 2016 by irrigation source type.

Source type	Irrigated acres	% pivot	% sprinkler	% flood
Groundwater	51,100	90.2	7.7	2.2
Combined groundwater and surface water	15,900	36.3	10.9	52.8
Surface water	70,500	1.1	0.4	98.5
Total	137,500	38.4	4.2	57.4

5.2.2. Mapping EvapoTranspiration at High Resolution with Internalized Calibration (METRIC) Model

The METRIC model was used to develop the monthly spatial ET maps for estimating historical agricultural ET rates and volumes in the GHVA for 14 calendar years starting in 1991 and ending in 2019. METRIC (Allen and others, 2007), is a thermal and optical ET model developed at the University of Idaho in conjunction with the Idaho Department of Water Resources and has been extensively applied for water management in the western United States. The METRIC model has been validated and compared with in-situ ET in Oregon and surrounding states. The main advantage of using thermal and reflectance data from Landsat imagery collected at 30 m resolution every 8 to 16 days is the ability to account for spatial and temporal variability in vegetation vigor and water stress at the field scale, the scale at which water rights are managed.

METRIC uses remotely-sensed optical and thermal data to estimate ET as a residual of the full surface energy balance (SEB):

$$LE = R_n - G - H \quad (3)$$

Where

- LE = latent heat flux consumed by ET (W/m²)
- R_n = net radiation from the sun, atmosphere, and surface (W/m²)
- G = heat flux into the ground (W/m²)
- H = sensible heat flux to the air (W/m²)

For estimating evaporation from open water areas where heat storage is difficult to estimate, the direct aerodynamic approach was applied within METRIC for pixels identified as open water (Allen et al., 2014; Appendix 10). The direct aerodynamic method has been shown to be accurate compared to measured

evaporation from eddy covariance and Bowen Ratio systems at American Falls in SE Idaho (Allen and Tasumi, 2005).

The METRIC model was applied using Landsat 5 Thematic Mapper (TM), Landsat 7 Enhanced Thematic Mapper Plus (ETM+), and Landsat 8 Operational Land Imager (OLI) satellite imagery. The TM, ETM+, and OLI images have a 30 m visible and shortwave pixel size while the thermal band pixel size is 120 m for TM and ETM+, and 100 m for OLI, spatial resolutions well-suited for estimating ET from individual fields in the western U.S. Each Landsat satellite has a 16-day repeat cycle with an offset of 8 days between each satellite, for a potential Landsat image available every 8 days, which in the western U.S. typically provides one clear usable image each month during the growing cycle to capture crop green up and harvesting cycles. The other data needed to run METRIC are a digital elevation model (DEM), land cover classification, and hourly and daily weather data to compute ETr. METRIC relies on local weather data from NLDAS to compute hourly ETr to calibrate ET estimates and the daily alfalfa ETr gridMET product to interpolate ET estimates in time, with ETr calculated using the ASCE standardized Penman-Monteith equation (ASCE-EWRI, 2005). A detailed description of the METRIC model and applications can be found in Allen et al., (2007a, b).

5.2.2.1. Overpass ET Calculation

METRIC solves for LE as the residual of equation (3) by first estimating R_n and G directly from satellite data, DEM, and land cover (Allen et al., 2007). Then H is estimated as a function of surface temperature and atmospheric stability using a one-dimensional bulk aerodynamic function:

$$H = \frac{\rho c_p dT}{r_{ah}} \quad (4)$$

Where

ρ	= air density (kg/m ³)
c_p	= specific heat of air at constant pressure (kJ/kg °C)
dT	= vertical near surface temperature difference (°C)
r_{ah}	= aerodynamic resistance (s/m)

Sensible heat flux (H) is solved by calculating dT for each pixel as a linear function of surface temperature (T_s). This iterative procedure is known as the Calibration using Inverse Modeling at Extreme Conditions (CIMIC).

The CIMIC procedure requires the selection of two “anchor” calibration pixels where LE can be easily estimated allowing equation 4 to be solved for H . These two anchor pixels represent extreme ET conditions in the image (upper and lower bound ET rates). H is approximated at the two extreme conditions T_s and dT can be applied to every pixel in T_s image to solve for H . Finally, R_n and G are computed allowing LE to be calculated using equation 3.

Calibration pixels for each Landsat image were selected manually using a combination of agricultural field boundaries, Landsat image raster data and METRIC generated outputs including: fraction of ET (ETrF), surface temperature, normalized difference vegetation index (NDVI), and surface albedo. The following section provides a brief description of the process, which is described in detail in the METRIC manual (Allen and others, 2014).

5.2.2.2. Pixel Selection Criteria

In general, the criteria used for the selection of the anchor pixels (also known as “hot” and “cold” pixels) were based on recommendations outlined in the METRIC documentation (Allen et al., 2007a, 2014). Hot and cold pixels were ideally selected in grid cells lying within the agricultural field boundaries so that the crop and soil properties of the selected anchor pixels represented agricultural conditions.

The “cold” pixel calibration point represents conditions of maximum ET rate where all of the available energy ($R_n - G$) is consumed by LE and H is zero. By default, this “cold” pixel was assigned the maximum ET rate set as the alfalfa-based reference ET (ETr) rate from NLDAS multiplied by the fraction of reference ET (ETrF) value of 1.05. Past studies have shown that the coldest, wettest agricultural fields in a satellite image, typically with a wet soil surface beneath a full cover alfalfa crop, tend to have an ET rate 5 percent above the alfalfa reference crop ET (Tasumi and others, 2005). Full cover alfalfa typically exhibits an NDVI range of 0.76 to 0.84 and surface albedo of 0.18 to 0.24. The cold pixel selection criteria are as follows: 1) an initial ETrF value greater than 1.05 that is assigned using the automated procedure (Allen and others, 2013), 2) NDVI greater than 0.76, 3) surface albedo between 0.18 and 0.24, and 4) location near center of the irrigated field (to avoid edge effects).

The “hot” pixel calibration point is representative of conditions with evidence of significant surface heating and minimal ET, ideally located in an agricultural field with bare soil and very little vegetation. Typically, this is represented where surface temperature, albedo, and vegetation indices are relatively homogeneous with respect to the agricultural field boundaries. By default, this “hot” pixel is assigned an ETrF value of 0.1. Based on the criteria in the METRIC manual, hot pixels selection criteria were as follows: 1) an initial ETrF value less than 0.1, 2) NDVI between 0.11 and 0.16, and 3) a surface albedo between 0.17 and 0.23.

Because images from early and late in the year don’t typically contain full cover crops, the NDVI and surface albedo criteria were relaxed for those cases. Instead, the pixel selection priority was to find hot and cold pixels with a minimum surface temperature difference of 4 °C.

5.2.2.3. Calculation of Daily and Seasonal ET

Once the CIMIC process was complete pixel-by-pixel R_n , G , H were computed and used to estimate LE at the time of image acquisition using equation 3. ET_{inst} (mm/hr) is then computed as:

$$ET_{inst} = 3600 \times LE_{inst} / \lambda \quad (5)$$

Where

LE_{inst}	= instantaneous latent heat flux derived from METRIC (W/m ²)
λ	= latent heat of vaporization for water (J/kg)
3600	= a factor for time conversion from seconds to hours

This value is used to compute the ratio of ET_{inst} to the alfalfa reference ET (ET_r) at the time of image acquisition, as the resultant ET fraction ($ET_rF = ET_{inst}/ET_r$), synonymous with the crop coefficient (K_c). ET_rF is computed for each pixel in the image. As described earlier, ET_r is computed using NLDAS weather data and the ASCE Penman-Monteith equation for an alfalfa reference (ASCE-EWRI, 2005), producing a 12-km grid for each image interpolated to the 30 m Landsat pixel scene. ET for the 24-hour period (ET_{24}) for a day is estimated as:

$$ET_{24} = \left(\frac{ET_{inst}}{ET_r} \right) ET_{r24} \quad (6)$$

Where ET_{r24} is the 24-hour reference ET for that day from the bias-corrected gridMET data. To estimate ET_{24} between image dates, linear interpolation of ET_rF is used and then multiplied by the gridded ET_r for each day to estimate daily ET_{24} per pixel. Linear interpolation is the default interpolation technique used in METRIC and was used in this application. Estimated ET for monthly, seasonal, and annual time periods is then computed as:

$$ET = \sum_{i=n}^m ET_rF \times ET_{24} \quad (7)$$

where n and m are the first and last days of the desired time period, respectively. The linear interpolation calculation is used to generate the 30 m summed ET raster maps at monthly and annual time steps, and tables of field-averaged ET data at daily, monthly, and annual time steps for each irrigated field.

5.2.2.4. Application and post-processing of METRIC model

This study used the open source Python implementation of the METRIC model (pyMETRIC v0.1.0) developed at the Desert Research Institute (DRI) to execute the equations described above. The code and documentation of workflow are available on the Western States Water Use Program (WSWUP)

GitHub webpage (<https://github.com/WSWUP/pymetric/releases/tag/v0.1.0>). The pyMETRIC algorithms and time integration were processed on local OWRD Windows PCs. Figure 6 illustrates a conceptual diagram of the datasets and workflow applied in this study.

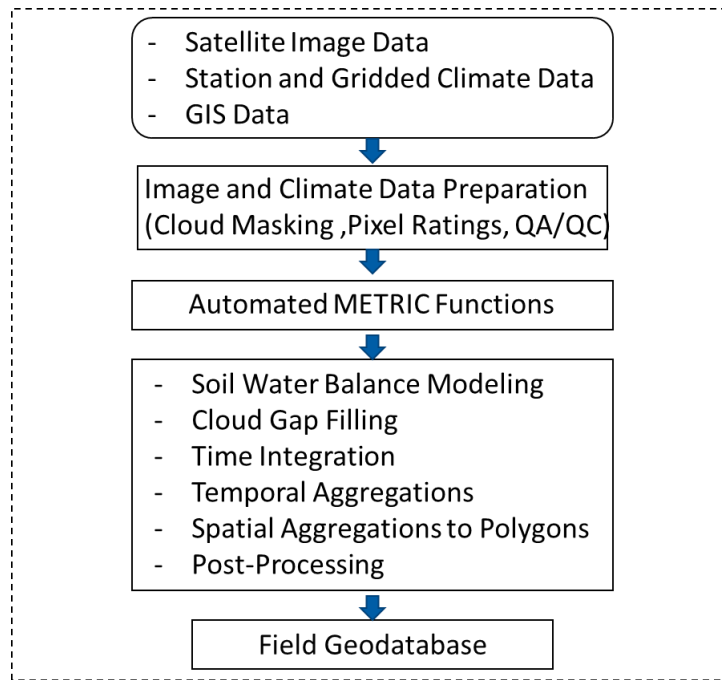


Figure 6. Conceptual diagram of datasets and workflow to generate field-level ET estimates using the METRIC model.

Quality assurance and control (QA/QC) of results was done using manual inspection of processed images and visualization of ET_rF histograms. Images with large populations of pixels above and below thresholds of 0.1 and 1.05 (the default lower and upper bounds of ET_rF) in agricultural areas indicated the initial pixels were not hot or cold enough. These images were re-calibrated by re-selecting hot and cold pixels until most of the pixels in agricultural fields had an ET_rF value within the upper and lower bounds. The ET_rF distribution was typically normally distributed or skewed towards the higher end during the growing season. Due to the large number of Landsat scenes being processed, typically only one pixel selection iteration was applied unless results did not converge.

Once the results were QA/QC'd for each image, rasters of monthly, seasonal (May - September) and annual totals of ET and precipitation were generated for the 14 analysis years. Rasters of monthly and seasonal ET estimates were spatially averaged to digitized annual field polygons to develop field-scale seasonal ET estimates. A 30 m inside buffer was applied to the field polygons prior to spatially averaging the ET rate to eliminate edge effects impacting the spatial average. Monthly, seasonal, and annual net ET rates were computed at the field-scale by subtracting gridMET precipitation estimates from spatially averaged ET estimates. It was assumed that the growing season net ET from an irrigated field represents the lower bound of crop water use because it assumes all precipitation is used for ET (100 percent effective). Finally, field-scale ET and net ET estimates were summarized by the irrigation source type classification. The area-weighted average ET and net ET rates for each irrigation source type

classification were calculated as the total ET or net ET volume divided by the total field acreage for all fields within each field classification.

5.2.2.5. Adjustment of METRIC ET datasets

A comparison between the METRIC and station ET for years 2018 and 2019 was made at daily and monthly time scales. First, daily station ET from the alfalfa EC station was compared with METRIC ET computed on the same day of the Landsat satellite overpass. Comparisons between the daily METRIC and station ET for the 25 overpass dates between March 2018 and August 2019 showed a fairly good correlation (r -squared = 0.9165; Figure 7) with METRIC ET being 16 percent higher than daily ET derived from the EC station.

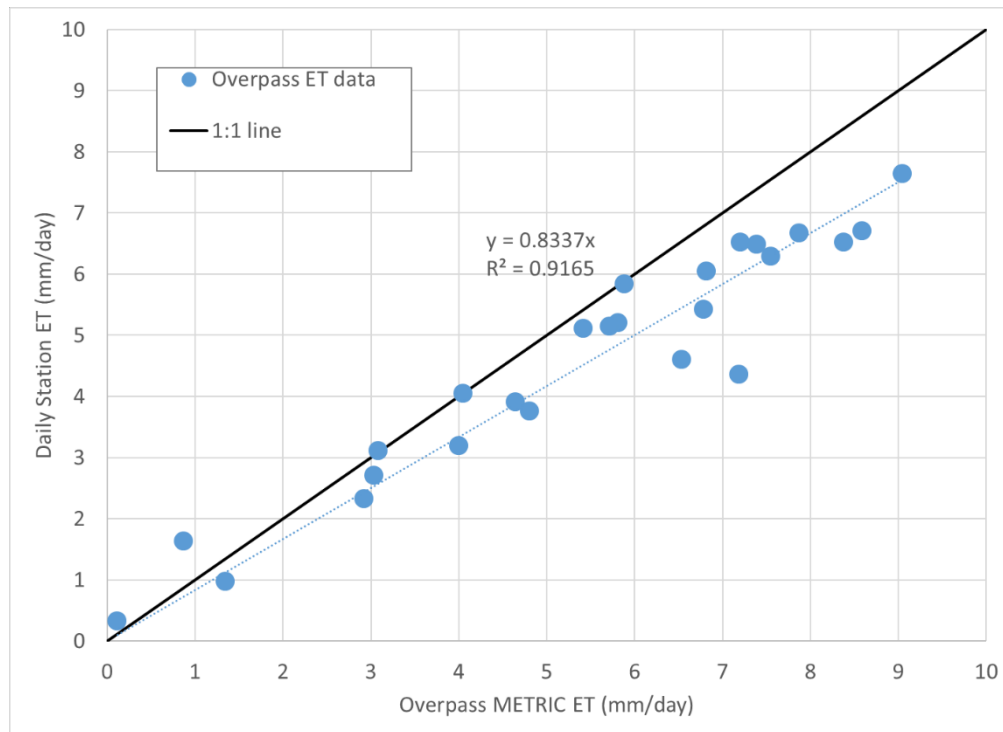


Figure 7. Scatterplot comparing daily (24-hr) ET at the Alfalfa ET station with METRIC daily ET on the 25 Landsat overpass dates between March 2018 and August 2019.

Station ET data was resampled to monthly sums and compared with monthly ET sums from the interpolated METRIC data for the 200-m footprint. The monthly METRIC data is generated using the linearly interpolated daily ETrF values and gridMET ETr data. The monthly ET data for the two years were averaged to create mean monthly measured and METRIC ET totals datasets. For the May-September time period, the adjustment factors ranged from 90 percent in May to 66 percent in September (Table 3), indicating METRIC ET consistently overestimated measured ET during the summer months for this field. The comparison of the seasonal total ET is shown for two growing season time periods in 2018 and 2019, indicating that station ET was about 79 percent of the METRIC ET totals (Table 4). In order to adjust the monthly and seasonal METRIC ET data, the monthly and seasonal ratios (Measured ET/METRIC ET in Table 4) were applied to adjust the METRIC ET data (both raster and tabular data).

Table 3. Mean monthly values for September 2017 to Aug 2019 time period.

Month	May	Jun	Jul	Aug	Sept	May-Sept
Measured ET (in)	4.9	5.4	6.9	6.0	3.5	26.7
METRIC ET (in)	5.4	7.1	8.0	7.8	5.3	33.7
Measured/METRIC (%)	90	76	86	77	66	79

Table 4. Seasonal total ET for two irrigation seasons at Alfalfa EC station.

Time period	May-Sept 2018	May-Aug 2019
Measured ET (in)	27.4	22.5
METRIC ET (in)	33.9	28.1
Measured / METRIC ET (%)	80.7	80.3

The cause of the overestimate of METRIC ET was investigated based on analysis of the daily ETrF time series from METRIC (blue line) and EC station (orange line) during the growing season (Figures 8 and 9). It was evident that the available Landsat overpass dates (black bars) during both 2018 and 2019 missed the majority of the alfalfa cuttings (green bars; 4 cuttings in 2018, 2 cuttings in 2019). Because the METRIC model linearly interpolates ETrF between Landsat overpass dates (blue line), this results in a consistent overestimate in the daily ET data between overpass dates when the cutting is missed due to sampling frequency. During periods where the sampling frequency captures the cuttings, the interpolated ETrF follows the measured ETrF more closely. This helps explain the overestimated METRIC ET, particularly in the months of June and August.

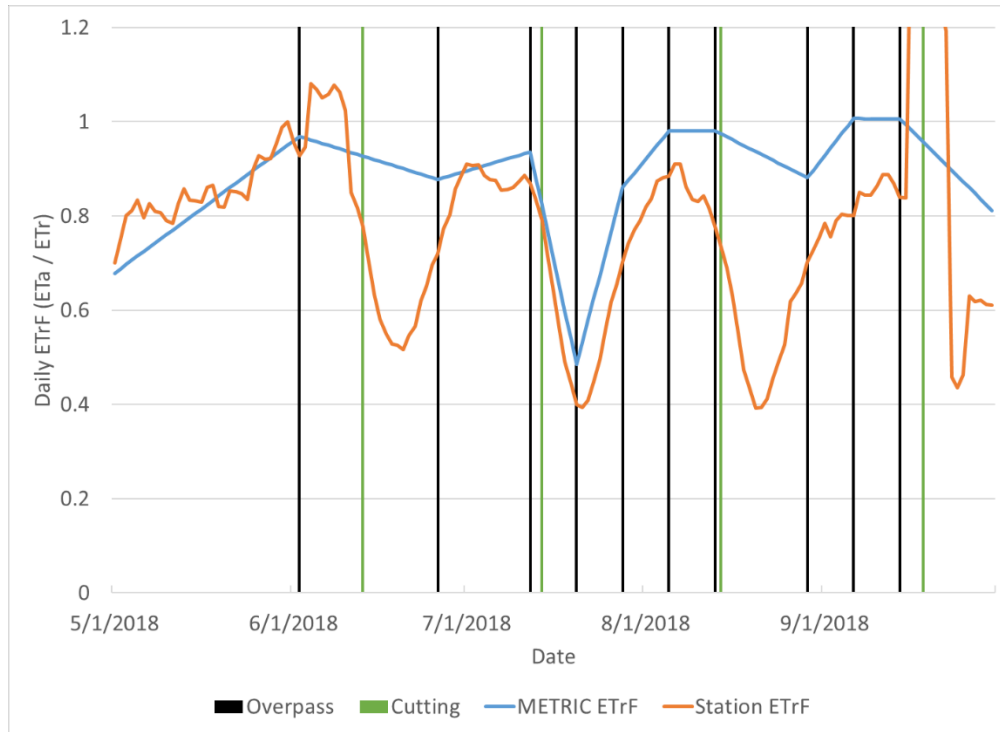


Figure 8. Plot showing daily time series of METRIC interpolated ETrF, CRN station ETrF, with overpass dates and reported field cutting dates for May-September 2018.

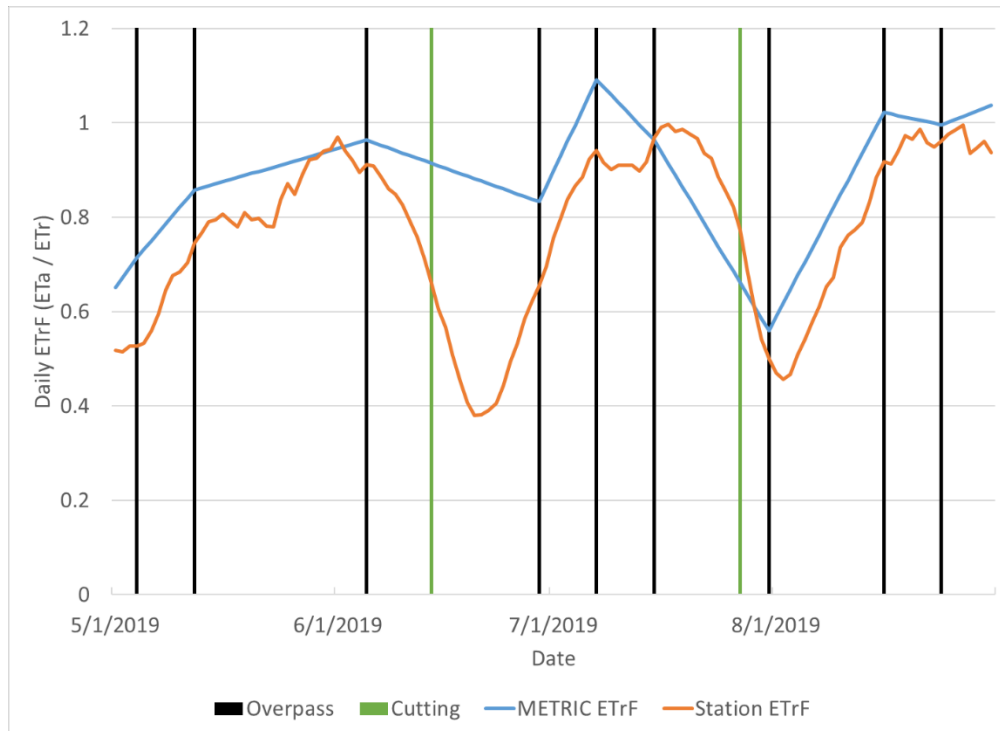


Figure 9. Plot showing daily time series of METRIC interpolated ETrF, CRN station ETrF, with overpass dates and reported field cutting dates for May-August 2019.

5.3. Estimation of Groundwater Pumpage

For fields irrigated with pumped groundwater, the seasonal pumpage volume (in acre-feet) can be estimated by dividing the seasonal net evapotranspiration (ET) rate (in feet) by the irrigation efficiency (%) multiplied by the area of the field (in acres):

$$\text{Pumping volume} = \frac{\text{Net ET rate}}{\text{Irrigation efficiency}} \times \text{Irrigated acres} \quad (8)$$

The State of Washington Department of Ecology defines irrigation efficiency as the ratio of crop water use to total applied water (irrigation efficiency = crop water use / total applied water) and provides the following irrigation efficiency ranges: surface flooding generally ranges from 35-60 percent (average 50 percent), sprinkler systems from 60-85 percent (average 75 percent), and center pivot systems from 75-95 percent (average 80 percent) (Washington State Department of Ecology, 2005). The Washington Department of Ecology also recommends computing basin-specific irrigation efficiency values using measured ET and applied irrigation water (in this case groundwater pumpage data) where available to confirm assumptions. The groundwater pumpage data is typically measured directly using totalizing flow meters, estimated indirectly from power meter data, or run-time and water right information.

While irrigation efficiency does vary with irrigation system and between fields, for this study it was assumed to be relatively consistent for the irrigation systems in the basin. In addition, based on the GIS assessment of irrigation systems, most groundwater irrigated fields use similar type irrigation systems (e.g. center pivot with mid-elevation spray application).

5.3.1. Validation with Pumpage Datasets

User reported pumpage volumes from irrigation wells were obtained from the OWRD Water Use Reporting (WUR) database (https://apps.wrd.state.or.us/apps/wr/wateruse_query/). This data is reported monthly for a select number of groundwater irrigation rights using a variety of measurement methods. For the user-reported pumpage data OWRD encourages users to report high quality data and has tools and processes for QC to screen the reported values.

Reported groundwater pumpage volumes from the WUR database were identified using the following criteria: 1) data tied to a groundwater irrigation water right in the GHVA, 2) pumpage volume was estimated using flow meters and volumetric methods, 3) data collected during 2014 to 2016, and 4) the irrigation well where the pumpage was estimated could be visually paired with the mapped irrigation field boundaries (typically 1-2 fields) where the pumped groundwater was applied. For each pumping well and year, the reported pumpage volume and irrigated acres were checked and any data appearing erroneous or from fields appearing to have supplemental contributions from ungaged sources was discarded. Pumpage data from 23 pumping well locations distributed across the GHVA was used.

In order to estimate the total groundwater pumpage based on remotely-sensed ET data, a locally derived value of irrigation efficiency, taken as the ratio of field-summed May to September net ET volume and reported pumpage volume, was determined for the select groundwater irrigated fields. Water user reported pumpage volumes at selected wells were paired with METRIC derived field-

summed adjusted net ET volumes for the fields where water was applied. METRIC output and pumpage data from the period 2014 to 2016 was compared.

Figure 10 is a scatterplot showing the reported seasonal pumpage volume (y-axis) and adjusted METRIC seasonal net ET volume (May-September net ET*acreage) (x-axis) for the 23 pumping wells located in Harney County during 2014 to 2016. The average irrigation efficiency (net ET volume / pumpage volume) for the 59 data points is 70 percent. The pumping wells used for this analysis supplied fields using the mid-elevation spray application (MESA) irrigation method on center pivot systems. For the full study period analyzed (1991 to 2018), MESA center pivots were assumed to represent the dominant irrigation method for primary groundwater irrigated fields in the basin. More recently (2017 to present) there has been an effort to install or convert to Low Energy Precision Application (LEPA) and Low Elevation Sprinkler Application (LESA) irrigation technology in an effort to increase efficiency and reduce pumpage (M. Owens, personal communication, April 24, 2019). Pumpage data from the 2014 to 2016 period was primarily applied used MESA systems and was assumed to be more representative of the long-term groundwater irrigation systems and rates in the basin.

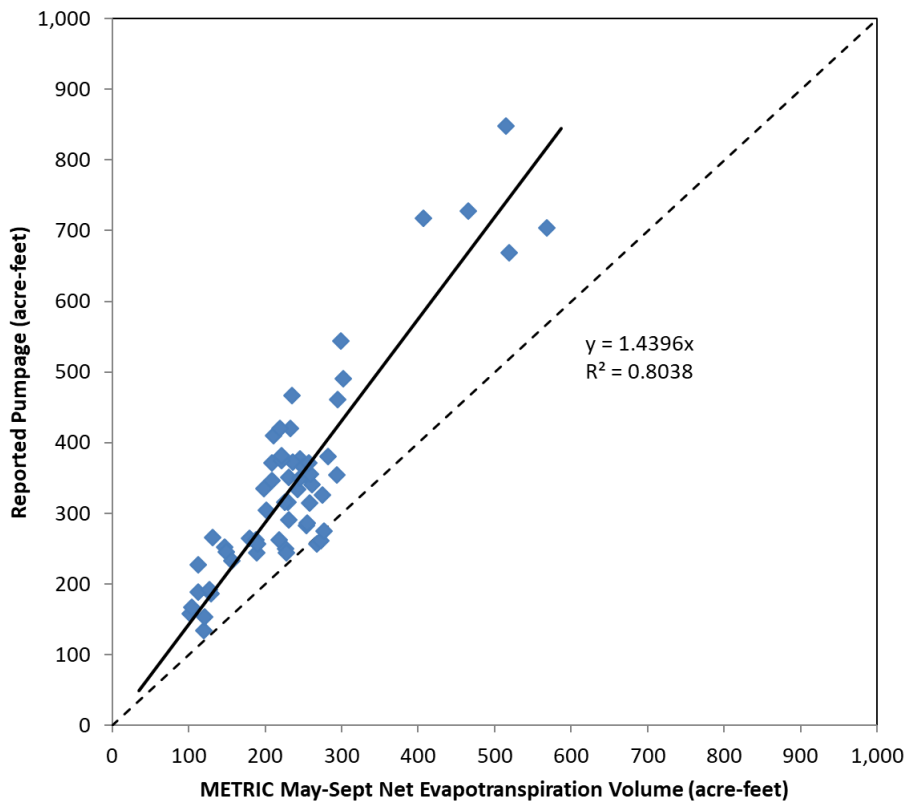


Figure 10. Scatterplot of METRIC field-scale seasonal ET volumes (x-axis) and reported seasonal pumpage volumes (y-axis) from 23 pumping well facilities in the Harney Basin for years 2014-2016.

Sarwar et al., (2019) found that for MESA-type irrigation systems in a similar environment (eastern Washington) that the fraction of applied water that reaches the soil surface was about 80 percent, indicating that about 20 percent of the applied water is lost to wind drift and surface evaporation. During the study period, MESA systems composed the majority of the center pivots in the study (M. Owens, personal communication, April 24, 2019). Based on the data collected and literature review, this indicates that on average for MESA systems in the Harney Basin, 70 percent of applied water is used up by ET, 20 percent goes to wind drift and surface evaporation, and 10 percent goes to runoff and deep percolation.

5.3.2. Water Budget Measurements – Case Example

As additional evidence for the relationship between ET and applied pumped groundwater, a summary was made of the measured water budget components (ET, precipitation, applied irrigation) for two irrigation seasons (2018 and 2019), based on the eddy covariance ET time series, precipitation data from the cumulative storage precipitation gage, and reported pumpage from the groundwater well supplying the center pivot system in the alfalfa field (Table 5). In addition to the seasonal totals, estimates of the field water balance (WBAL= applied irrigation + precipitation – ET), irrigation efficiency (net ET / irrigation), and percent residual (WBAL / applied irrigation) were included. These measured water budget components help support and ground-truth the remotely-sensed ET estimates.

Table 5. Measured irrigation (IRR), precipitation (PPT), and evapotranspiration (ET) totals from the Harney Alfalfa EC station, years 2018 and 2019

Irrigation season	IRR* (in)	PPT** (in)	ET*** (in)	WBAL = IRR + PPT – ET (in)	(ET-PPT) / IRR (%)	WBAL / IRR (%)
May-Sept 2018	30.7	2.0	27.4	5.3	83%	17%
May-Aug 2019	27.9	2.7	22.5	8.1	71%	29%

Data sources:

* Reported water use volume divided by reported area (125 acres); totalizing flow meter; irrigation season 2018 was 4/24 to 9/9 and for 2019 5/4 to 8/28

** Cumulative precipitation from storage precipitation gage located at center of field

*** Station ET data from eddy covariance flux measurements gap filled and energy balance corrected

Results indicate an application efficiency of 70 to 80 percent and a residual of 20 to 30 percent that is likely lost to a combination of deep percolation, runoff, and wind drift. Considering uncertainty and error within each measured term, the computed application efficiency is fairly typical for a low elevation sprinkler application (LESA) system at the field scale.

5.3.3. Pumpage from Fields Irrigated with Groundwater and Surface Water

Very few water use records (surface water or groundwater) exist for fields irrigated with both diverted surface water and groundwater pumping. Previous studies have generally addressed this by assuming that the supplemental groundwater composes a proportion of the total crop water requirement or duty for an irrigated field. For example, in both the Willamette and Upper Klamath groundwater hydrology reports the authors assume that pumped supplemental groundwater accounted for 50 percent of the

irrigation crop water requirement from those lands (Conlon and others, 2005; Gannett and others, 2007). In the Nevada Department of Water Resources 2015 report “Statewide Groundwater Pumpage Inventory” the groundwater pumpage permitted or certificated as a supplemental right to surface water was estimated to be 75 percent of the duty for the statewide groundwater pumpage estimates (State of Nevada Division of Water Resources, 2017). The 75 percent value was for a dry year (2015) and for the wetter year 2017 a value of 50 percent was used (A. Sullivan, personal communication, 2019). A value of 90 percent from supplemental pumpage was assumed for the Humboldt River basin in 2015 due to shortage of surface water and drought conditions.

In the Harney Basin one of the few locations with supplemental groundwater pumpage information from a field irrigated with supplemental groundwater is located at the Eastern Oregon Agricultural Research Station (EOARC) in the Silvies River Floodplain. This location has an older primary surface water right (1926 Silvies River decree, priority date 1886) and supplemental groundwater right (Certificate 44592, priority date 1968) that has groundwater pumpage reported concurrently with METRIC from 2014 to 2016. This 60-acre field has a grass / alfalfa mix planted, uses a wheel line sprinkler irrigation system to irrigate with pumped groundwater (well ID: HARN 852), and is surrounded by extensive flood irrigation and very shallow groundwater levels (<5 ft bls). Based on the adjusted METRIC net ET volume and reported pumpage, a ratio of crop water use derived from pumped groundwater can be estimated as:

$$\text{Ratio of ET from GW} = \frac{\text{GW Pumpage} \times \text{Irrigation Efficiency}}{\text{Total crop ET}} \quad (9)$$

At this location the adjusted net ET represents both groundwater and surface water irrigation sources. In order to estimate the portion from just groundwater, equation 9 was applied using the reported pumpage and a 70 percent irrigation efficiency estimate (Table 9). The average contribution from groundwater pumping to total ET for 2014 to 2016 is 47 percent, very similar to the 50 percent assumption in the previous studies (Conlon and others, 2005; Gannett and others, 2007).

Table 6. METRIC adjusted net ET volume, reported pumpage, and estimated portion of ET from pumped groundwater from field irrigated by well HARN 852 for 2014-2016 at EOARC.

Variable	2014	2015	2016	3-year avg.
METRIC Net ET Volume (ac-ft)	97.3	99.7	124.4	107.1
Reported water use from irrigation well HARN 852 (ac-ft)	74.2	68.5	72.1	71.6
Estimated crop water use from GW pumping (ac-ft; assuming 70% irrigation efficiency)	51.9	48.0	50.5	50.1
Ratio of crop water use from GW to METRIC net ET volume (%)	53	48	41	47

The data presented in Table 6 data from this location supports the assumption that 50 percent of the net ET volume for fields irrigated with both surface water and groundwater is from pumped groundwater. Given that most of the fields irrigated with surface water and groundwater are located within a floodplain and there is only one site for comparison, the value could vary either way depending on surface water availability.

5.3.4. Regional Groundwater Pumpage Estimates

For fields irrigated with groundwater, it was assumed that 100 percent of the crop water use was from pumped groundwater with an average efficiency of 70 percent. For fields irrigated with groundwater and surface water, it was assumed that 50 percent of the crop water use was supplied by pumped groundwater with an average efficiency of 60 percent. The lower efficiency value for supplemental groundwater irrigation systems was assumed based on the GIS assessment presented in Table 2 which indicated that these fields irrigated with lower efficiency systems (flood and sprinkler) than the pivots systems used to irrigated primary groundwater fields.

In order to estimate total groundwater pumpage for each year and sub-region, the monthly adjusted METRIC net ET volumes for each field irrigated with either groundwater or groundwater and surface water was first multiplied by the percent of pumped groundwater (100% for GW only fields, 50% for combined SW & GW fields), then divided by the assumed irrigation efficiency (70% for GW only fields, 60% for combined SW & GW fields). Months with negative adjusted net ET volumes were set to zero to avoid negative pumpage volume. The monthly pumpage volume for each field was summed to seasonal totals. Lastly, the field-level groundwater pumpage volumes were summed by region to get regional totals for each year.

6. RESULTS

This section describes the results used to estimate historical crop ET rates and volumes and groundwater pumpage for irrigation in the GHVA. This includes the following components: 1) monthly and seasonal adjusted METRIC ET rates for the 13 years analyzed between 1991 through 2018 for all fields in the study area summarized by irrigation source type, and 2) monthly and annual estimated groundwater pumpage. The final groundwater withdrawal estimate is based on the mean annual value for the most recent 5-year period (2014 to 2018).

6.1. Crop Water Use Rates

Monthly, seasonal, and annual rasters of ETr, PPT, adjusted METRIC ET, and net ET (adjusted METRIC ET minus PPT) were generated for each of the 13 years processed for the entire GHVA area and summarized by irrigation source type. Seasonal May through September net ET clipped to irrigated fields is shown in Figure 11 for 1991 and Figure 12 for 2018. Each figure demonstrates the spatial ET variation within individual fields and different parts of the valley. Mean May-September net ET depths for all mapped fields was 1.3 feet for 1991 and 1.6 feet for 2018, and ranged from nearly 0 feet in unirrigated areas to 2.6 feet (similar to ETr) in groundwater irrigated center pivot fields and 3.1 ft in flood-irrigated areas in the MNWR.

Agricultural fields used for this analysis are delineated by the irrigation source types shown in Figure 13 for 1991 and Figure 14 for 2018. The comparison of ET and irrigated acreage shows the large increase in water use (Figures 11 and 12) and irrigated areas (Figures 13 and 14) from 1991 to 2018. Groundwater irrigated acreage shows an increasing trend over the observed period. The number of groundwater irrigated lands ranges from a minimum in 1991 of 20,200 acres for groundwater irrigated fields and 10,400 acres for groundwater and surface water irrigated fields (30,600 acres total), to a maximum in 2018 of 57,900 acres for groundwater and 16,200 acres for groundwater and surface water (74,100 acres total), representing an increase of 43,500 acres irrigated with groundwater (Figure 15). Fields irrigated with surface water (non-MNWR) have more year to year variability due to precipitation and runoff but lack a strong increasing trend, and average around 66,000 acres, whereas the irrigated fields on the MNWR were assumed to remain constant at 46,300 acres per year.

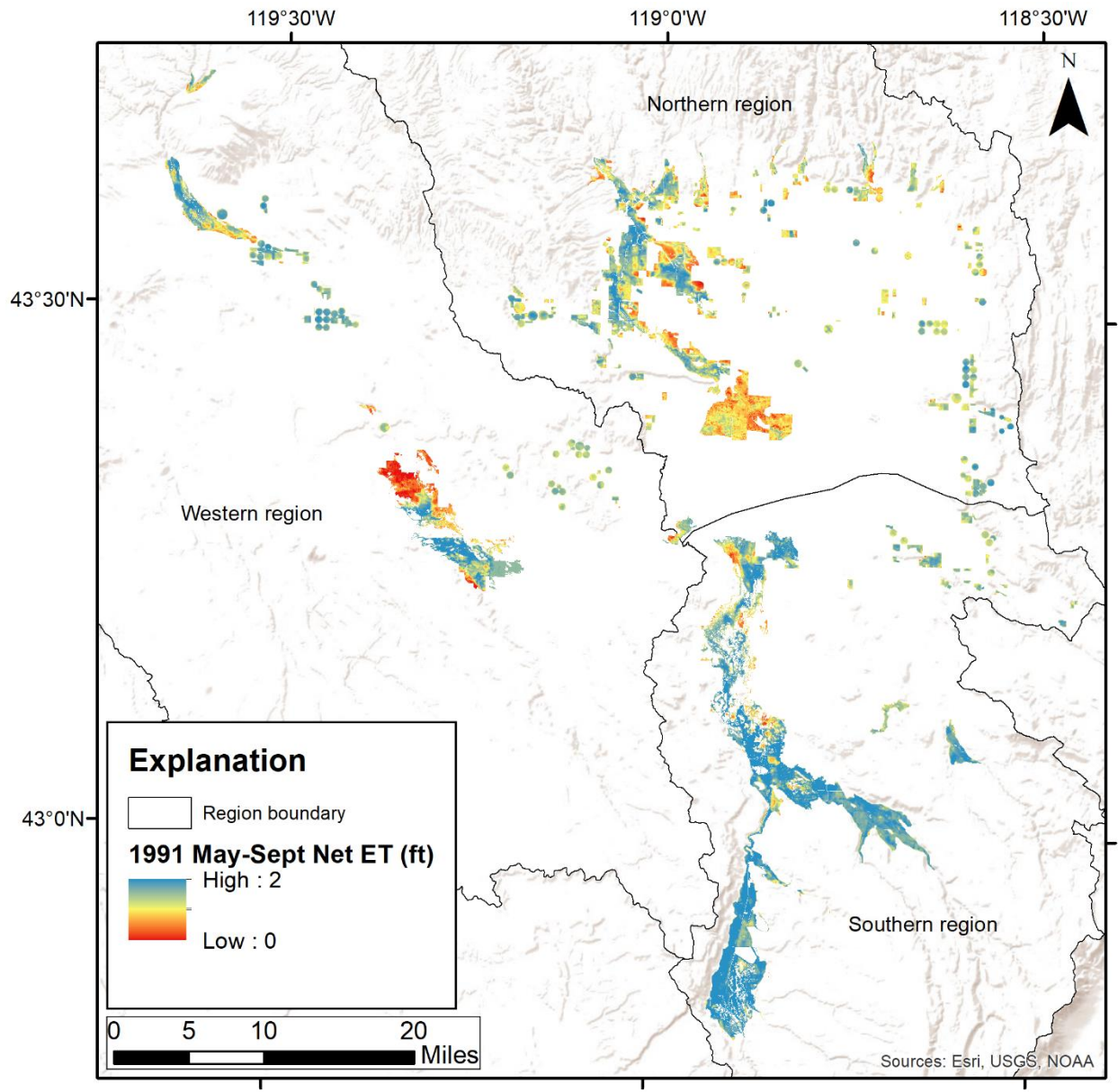


Figure 11. Net ET for Harney Basin, May-September 1991.

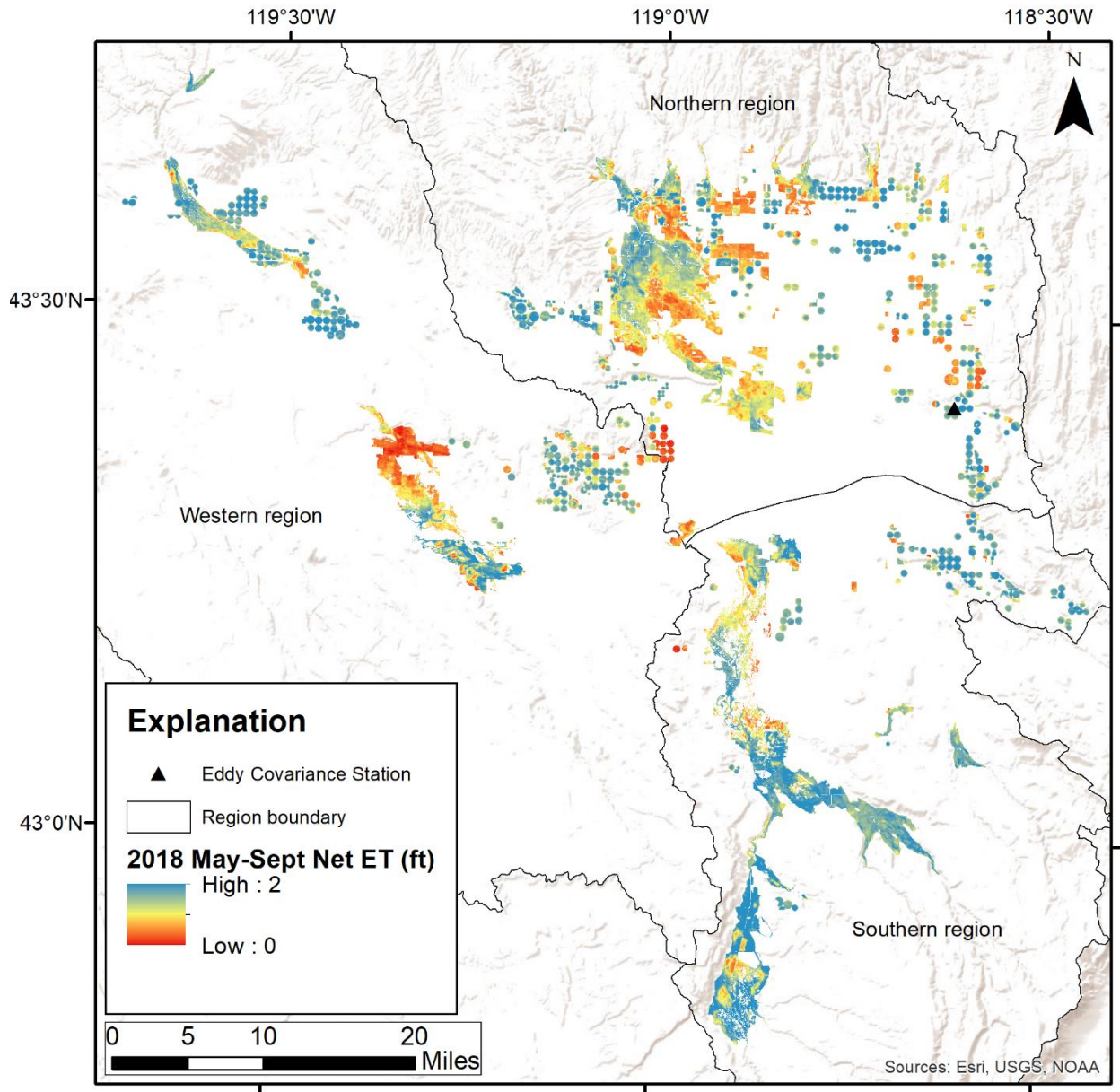


Figure 12. Net ET for Harney Basin and location of ET station, May-September 2018.

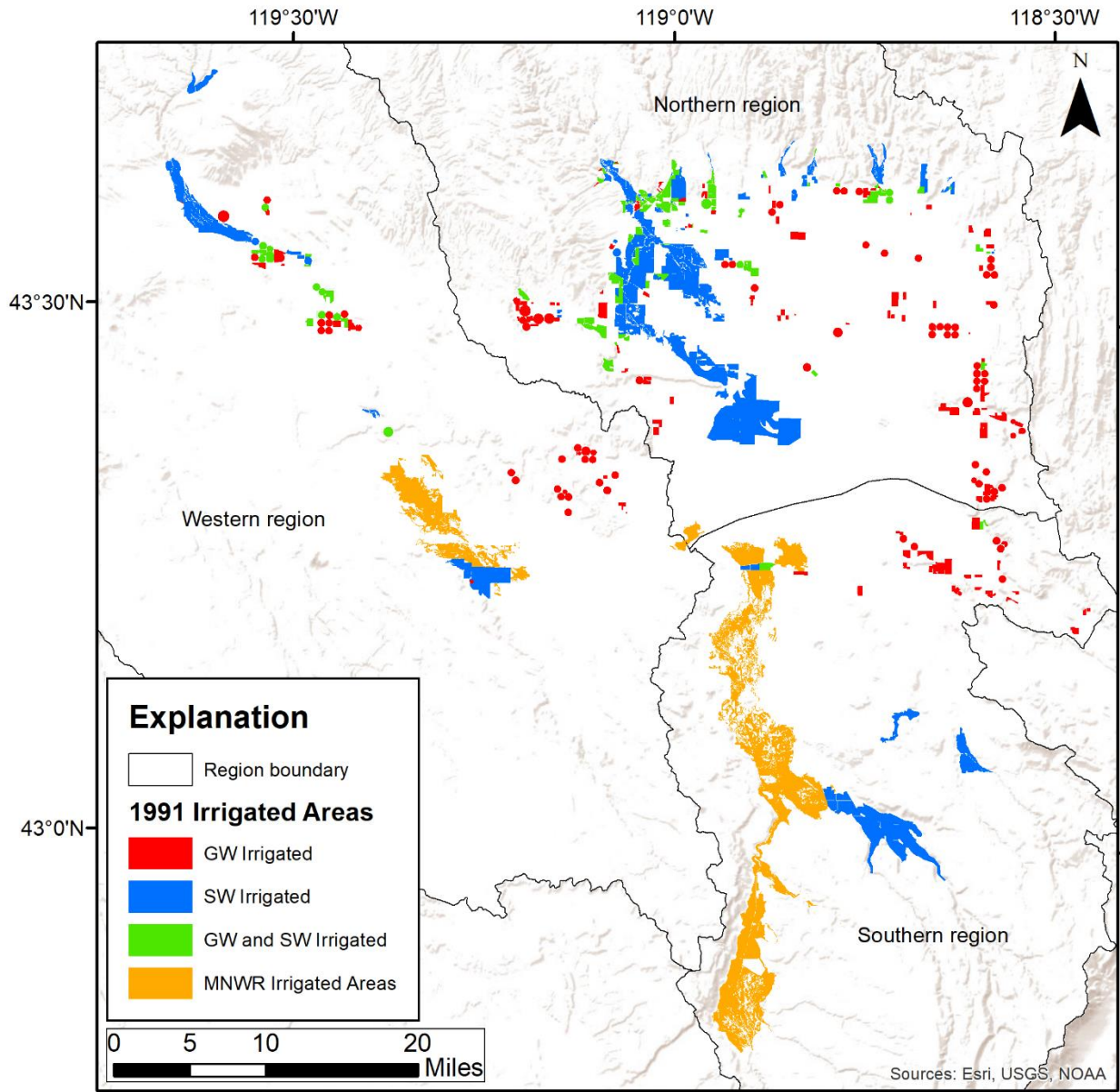


Figure 13. Irrigated fields by irrigation water source type, Harney Basin, 1991.

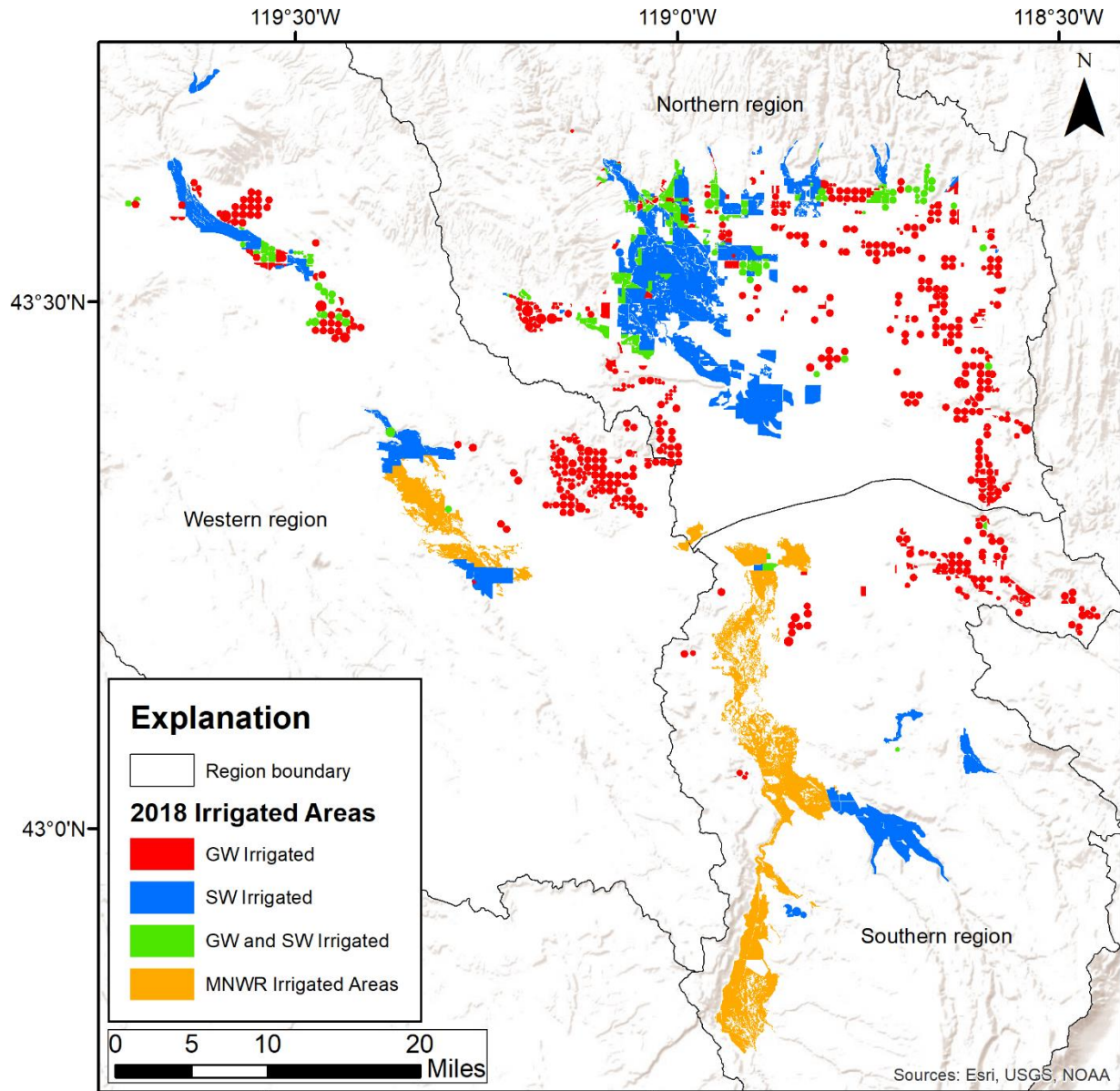


Figure 14. Irrigated fields by irrigation water source type, Harney Basin, 2018.

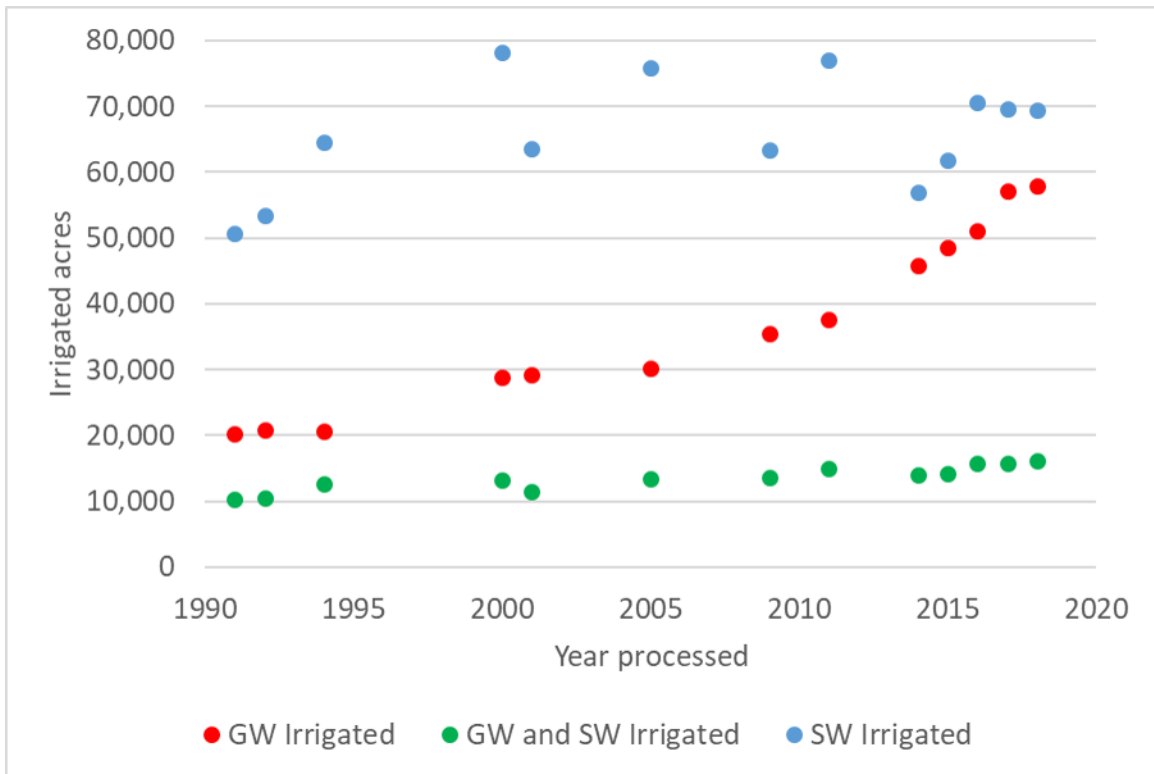


Figure 15. Annual time series of summed irrigated acres in the Harney Basin for all irrigated fields, except the MNWR, by irrigation water source type.

Area-weighted seasonal (May through September) net ET rates for irrigated fields identified by water source type are shown in Tables 7 and 8. The mean area-weighted seasonal net ET rates was 1.34 ft yr⁻¹ for surface water irrigated crops, 1.49 ft yr⁻¹ for fields irrigated with both surface water and groundwater, 1.51 ft yr⁻¹ for fields irrigated with groundwater, and 1.54 ft yr⁻¹ for surface water irrigated fields in the MNWR. Over the 13 years analyzed, the mean net ET rates for fields irrigated with surface water were more variable (standard deviation = 0.23 ft yr⁻¹) than those irrigated with groundwater (standard deviation = 0.14 ft yr⁻¹), reflecting inter-annual variability in surface water supply (Table 7).

Table 7. May through September Net Evapotranspiration Rates, in feet, by irrigation source type

YEAR	Groundwater	Groundwater and surface water	Surface water – non-MNWR	Surface water - MNWR
1991	1.36	1.34	1.30	1.60
1992	1.51	1.31	0.86	1.37
1994	1.67	1.41	1.36	1.81
2000	1.60	1.60	1.49	1.73
2001	1.59	1.49	1.19	1.86
2005	1.25	1.38	1.34	1.41
2009	1.42	1.53	1.50	1.26
2011	1.35	1.44	1.55	1.74
2014	1.75	1.69	1.46	1.54
2015	1.48	1.40	1.06	1.08
2016	1.63	1.64	1.47	1.43
2017	1.56	1.75	1.74	1.76
2018	1.46	1.37	1.14	1.46
Mean	1.51	1.49	1.34	1.54
StDev	0.14	0.14	0.23	0.24

Table 8. Mean seasonal May through September net evapotranspiration and pumpage rates by irrigation source and region, 1991-2018, Harney Basin, Oregon.

Irrigation source	Mean seasonal net evapotranspiration rate (feet/year)			
	Northern Region	Southern Region	Western Region	Harney Basin
Groundwater	1.48	1.51	1.57	1.51
Groundwater and surface water	1.44	1.60	1.66	1.49
Surface Water – non-MNWR	1.27	1.64	1.33	1.34
Surface Water – MNWR	1.04	1.64	1.23	1.54
	Mean seasonal pumpage rate (feet/year)			
Groundwater	2.12	2.15	2.24	2.16
Groundwater and surface water	1.20	1.34	1.38	1.24

Comparisons of cumulative mean monthly ET and precipitation rates highlight the relation between ET and precipitation over the water year and the onset of irrigation (Figure 16). Cumulative monthly precipitation exceeds ET until April, and cumulative crop ET exceeds precipitation from about April to September. This indicates that on average, ET from October to April is largely comprised of soil moisture supplied by winter precipitation rather than irrigation water, whereas ET during May through September is primarily attributed to irrigation. This is also supported in the reported water use data, where majority of reported pumpage began in May and ended in September. In all cases, July was the

month of maximum ET and net ET rates for all source types. The rate of decline after is sharper for the surface water irrigated fields as floodwater subsides and streamflow declines.

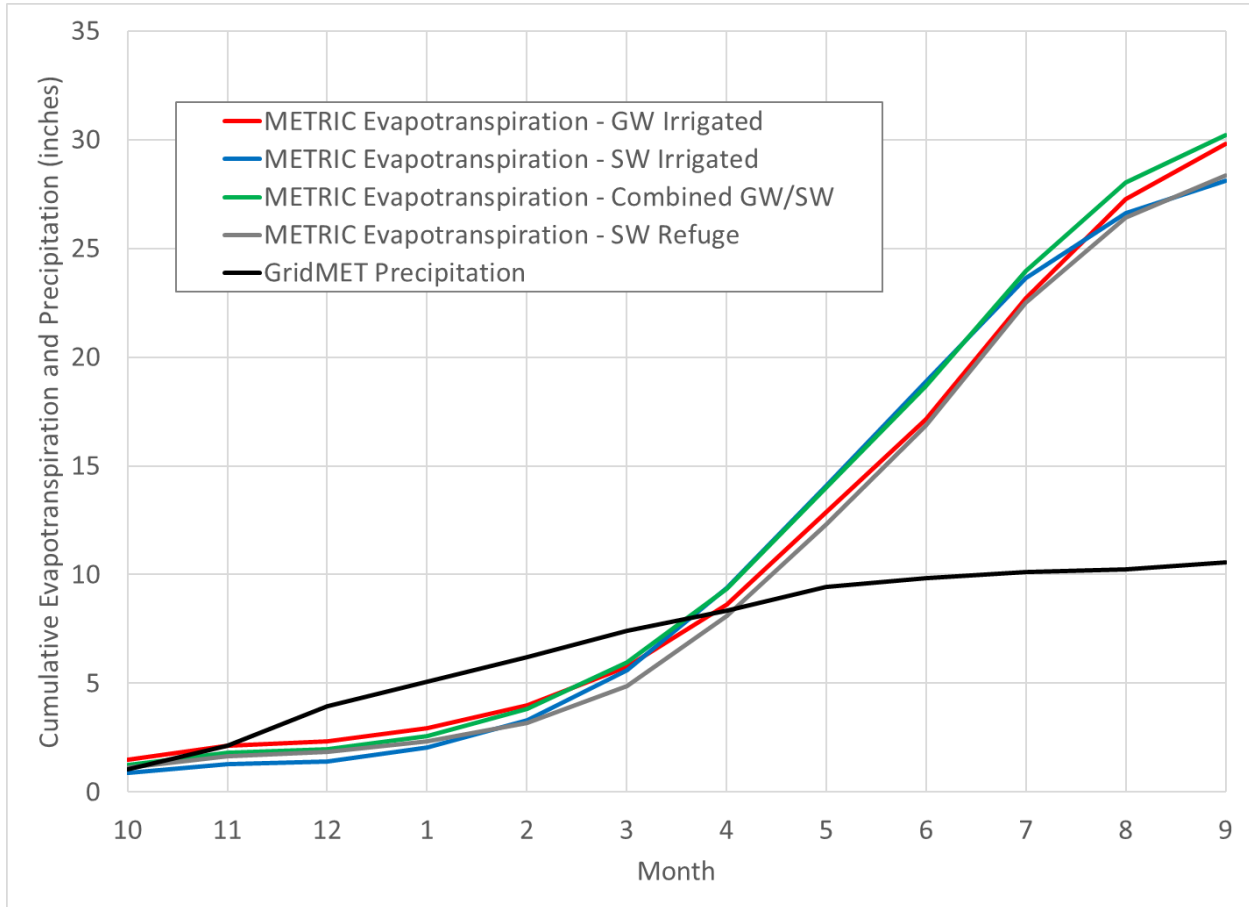


Figure 16. Spatially averaged mean cumulative water year adjusted METRIC ET and gridMET precipitation for years 2014-2018 by irrigation water source type, Harney Basin, Oregon.

6.2. Crop Water Use Volumes

The seasonal net ET volume by irrigation source type for the 13 analyzed years from 1991 to 2018 shows the combined influence of the inter-annual change in irrigated acreage and area-weighted net ET rates on annual ET volume (Figure 17). As reflected in the more variable irrigated acreage and net ET rates, the net ET volumes for the surface water irrigated fields have the largest inter-annual variability in the group. The surface water irrigated net ET volume increases from the early 1990’s (a very dry period) to early 2000’s with a minimum of 46,000 acre-feet in 1992 and maximum of 121,000 acre-feet in 2017. For groundwater irrigated fields the trend is upward starting around 30,000 acre-feet in the early 1990s to 80,000 acre-feet in the most recent 5-year period.

The average seasonal net ET volume from the most recent 5 years (2014 to 2018) of ET data is 260,000 acre-feet for all irrigated fields, with 82,000 acre-feet derived from groundwater irrigation, 24,000 acre-

feet from fields with combined surface water and supplemental groundwater, 91,000 acre-feet from surface water irrigation outside the MNWR, and 67,000 acre-feet from surface water irrigated portions of the MNWR (Table 9). About 9,260 acres irrigated by surface water on the MNWR in the Western Region (Figures 13 and 14) are typically irrigated with spring discharge rather than surface water from Silver Creek. The net ET of spring discharge from this area averages about 11,000 acre-feet per year, or about 16 percent of the net ET volume from the MNWR.

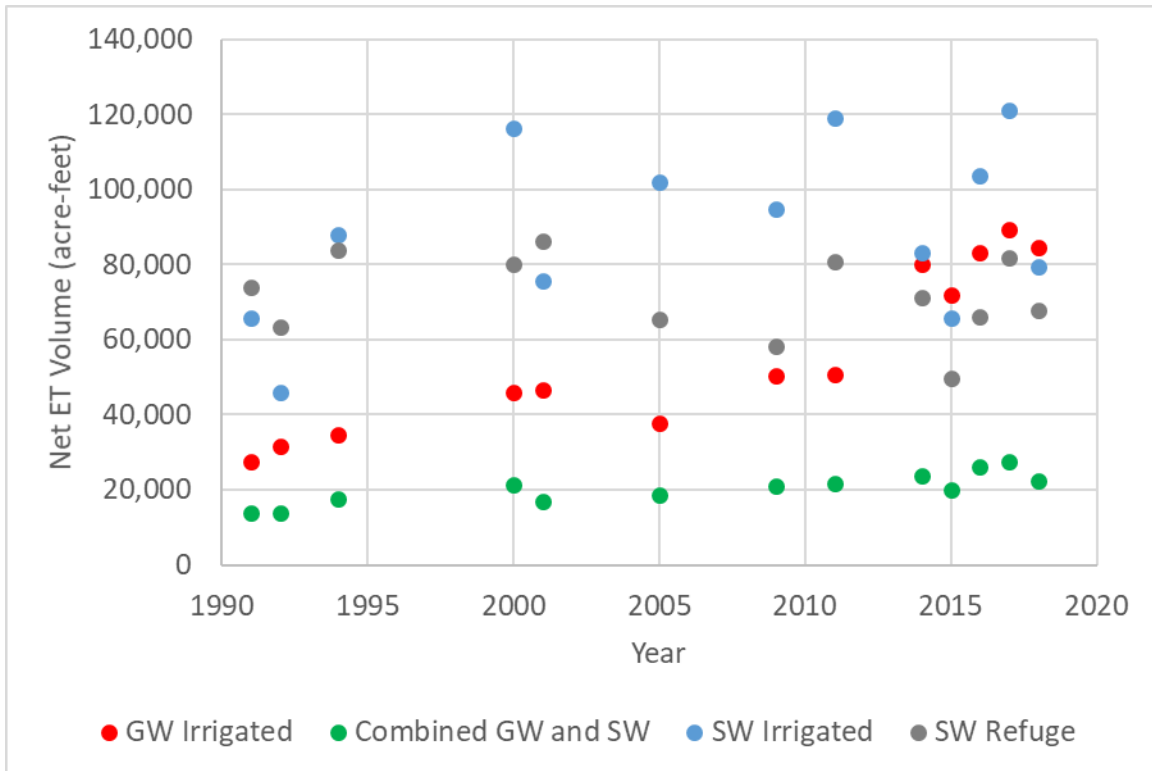


Figure 17. Time series of annual net evapotranspiration volume from irrigated areas by irrigation source type, Harney Basin, Oregon.

Table 9. May to September Net ET Volumes, in acre-feet x 1000, by irrigation source type

YEAR	Groundwater	Groundwater and surface water	Surface Water – non-MNWR	Surface water - MNWR	Total
1991	27.5	14.0	65.7	74.1	181.3
1992	31.5	13.7	46.0	63.5	154.7
1994	34.6	17.7	88.0	83.7	224.0
2000	45.9	21.3	116.4	80.2	263.8
2001	46.7	17.0	75.5	86.2	225.5
2005	37.8	18.5	101.9	65.3	223.5
2009	50.4	20.9	95.0	58.3	224.6
2011	50.6	21.5	119.1	80.7	271.9
2014	80.1	23.9	83.2	71.3	258.5
2015	72.0	19.9	65.7	49.8	207.4
2016	83.1	26.1	103.7	66.1	278.9
2017	89.2	27.6	121.2	81.6	319.5
2018	84.4	22.3	79.5	67.7	253.9
2014-2018 Average	81.8	23.9	90.6	67.3	263.7

6.3. Groundwater Pumpage Volumes

The plot of basin-wide estimated groundwater pumpage from groundwater irrigation indicates that between the early 1990s (1991 to 1992) and current (2017 to 2018) the total groundwater pumpage for irrigation for the Harney Basin increased from about 54,000 AFY (acre-feet per year) to 145,000 AFY, an increase of 91,000 AFY (170 percent) (Figure 18). The largest rates of change was due to a rapid increase in primary groundwater irrigation during early 1990s and 2000 and then 2011 to 2014. Pumpage remains steady from 2000 to 2010. The pumpage generally continues to increase during 2014 to 2018. Supplemental groundwater irrigation ranges from 12,000 acre-feet to 23,000 acre-feet but remains relatively stable during the time period 2000 to 2018. Supplemental groundwater irrigation accounts for a smaller fraction of the total pumpage for years 2014 and later (~15 percent) than the years 2000 and before (~20-25 percent).

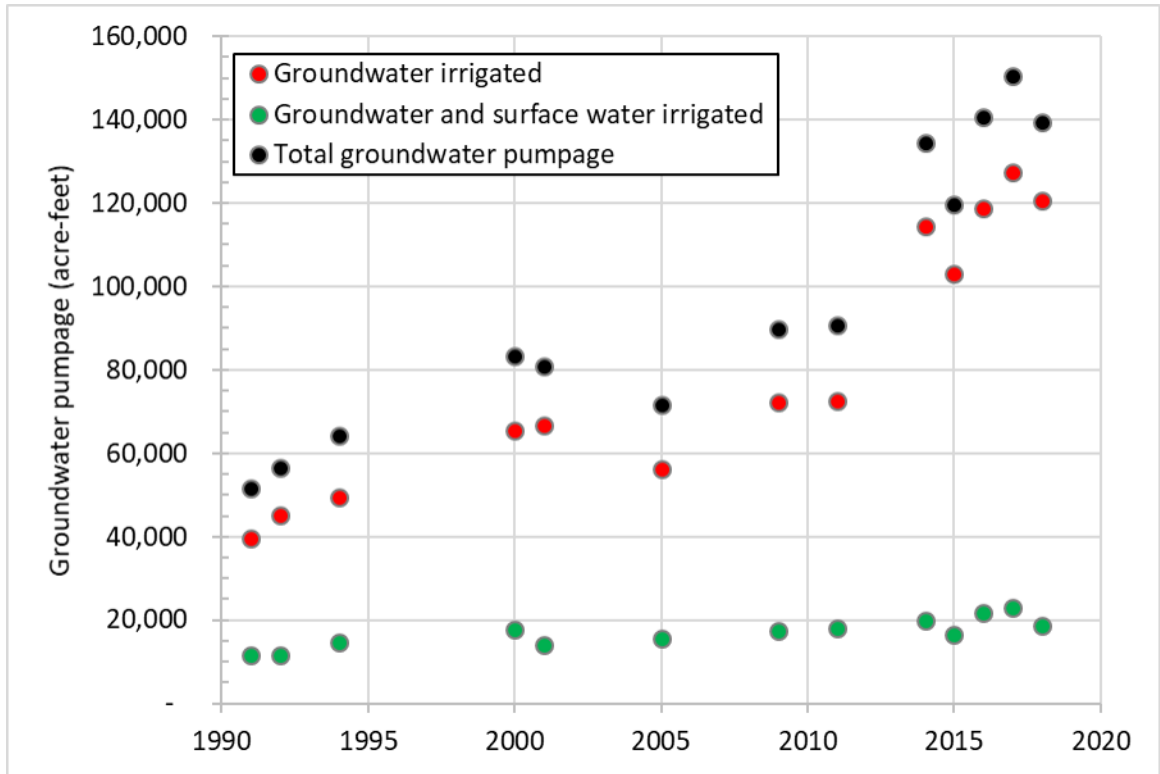


Figure 18. Time series of groundwater pumpage in the Harney basin from 1991 to 2018.

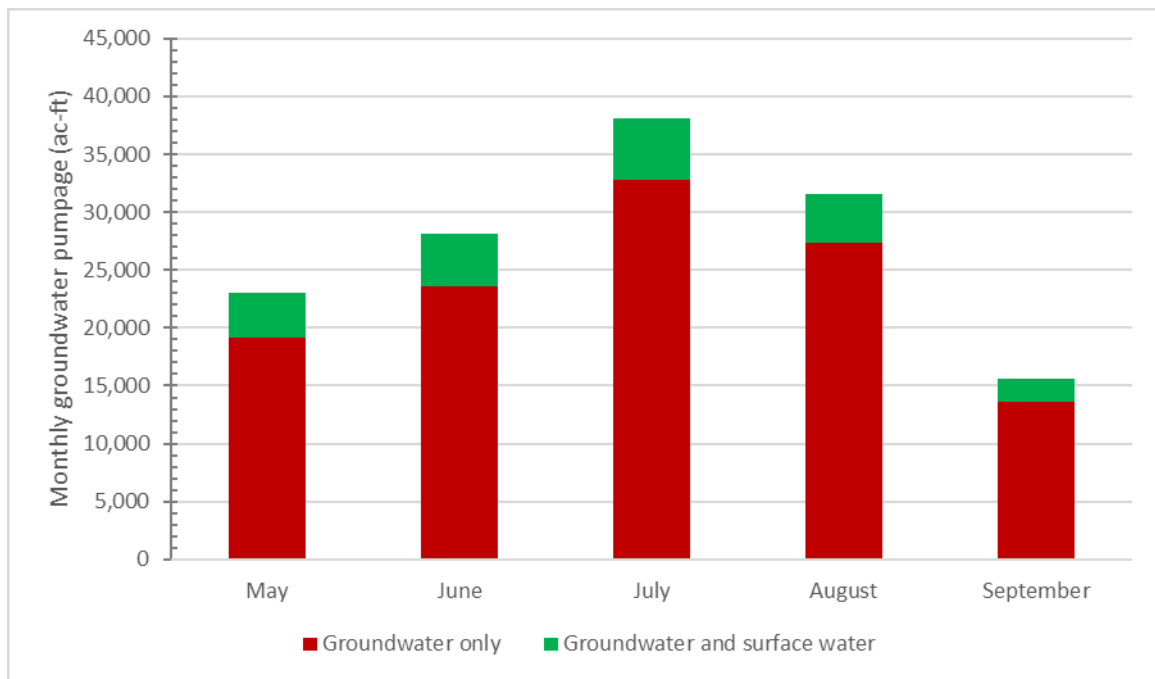


Figure 19. Mean monthly groundwater pumpage volume for 2014 to 2018 for fields irrigated with groundwater only and combined groundwater and surface water.

Groundwater pumpage peaks in July with an average of 38,000 acre-feet of groundwater pumpage to a minimum of 15,000 acre-feet in September (Figure 19). Groundwater only irrigation accounts for the majority of the pumping. Seasonal pumpage estimates for all years are summarized in Table 10.

Table 10. Total estimated seasonal groundwater pumpage from agricultural irrigation wells, Harney Basin, Oregon.

Total Seasonal groundwater pumpage: Computed as the ratio of net crop evapotranspiration and irrigation application efficiency (assumed 70 percent for fields with groundwater only and 60 percent for fields with both groundwater and surface water). Combined pumpage represents groundwater pumpage from fields irrigated by both groundwater and surface water (assumed 50 percent of supplied water from groundwater).

Year	Groundwater only GW Pumpage (acre-feet)	Groundwater and Surface Water GW Pumpage (acre-feet)	Total Groundwater Pumpage (acre-feet)
1991	40,000	12,000	52,000
1992	45,000	12,000	57,000
1994	49,000	15,000	64,000
2000	66,000	18,000	83,000
2001	67,000	14,000	81,000
2005	56,000	16,000	72,000
2009	72,000	17,000	90,000
2011	73,000	18,000	91,000
2014	110,000	20,000	130,000
2015	100,000	17,000	120,000
2016	120,000	22,000	140,000
2017	130,000	23,000	150,000
2018	120,000	19,000	140,000

For the groundwater budget and management, it is useful to break up the pumpage estimates from Harney Basin into three regions: Northern region, Southern region, and Western region. Groundwater irrigated and combined fields within each region were identified and summed together to get an annual total for each year (Table 11). Based on this information, an estimate of groundwater pumpage through time and relative to published recharge estimates (Garcia and others, 2021) can be computed. The 5-year average from 2014 to 2018, the most recent period with ET data processed, was computed to represent the current groundwater pumpage estimate. The mean annual pumpage estimates for each watershed are as follows: 76,000 acre-feet for the Northern region; 20,000 acre-feet in the Southern region; and 41,000 acre-feet in the Western region. The average total groundwater pumpage estimate for the GHVA area from 2014-2018 was 140,000 acre-feet per year.

Table 11. Total estimated groundwater pumpage by major drainage basin in GHVA, for select years between 1991 and 2018 and averaged for 5-year period 2014 to 2018.

Year	Northern Region	Southern Region	Western Region	Total
1991	32,000	7,200	12,000	52,000
1992	34,000	8,800	14,000	57,000
1994	40,000	9,400	15,000	64,000
2000	51,000	8,400	24,000	83,000
2001	47,000	9,600	24,000	81,000
2005	42,000	9,100	21,000	72,000
2009	53,000	12,000	25,000	90,000
2011	54,000	13,000	24,000	91,000
2014	74,000	20,000	41,000	130,000
2015	65,000	18,000	37,000	120,000
2016	79,000	21,000	41,000	140,000
2017	85,000	22,000	44,000	150,000
2018	77,000	22,000	41,000	140,000
5 yr Avg (2014-2018)	76,000	20,000	41,000	140,000

7. DISCUSSION

The methods to estimate ET and groundwater pumpage are not absent of uncertainties and limitations. Potential sources of uncertainty include calibration of METRIC and parameters used in the energy balance equation, uncertainty and biases in estimated reference ET and precipitation from gridded weather products, errors and data quality of observed weather datasets, errors in Landsat reflectance and radiance, issues with scene availability and time integration of ETrF in between Landsat images, errors in field polygon mapping and irrigation status attribution, errors and data quality in eddy covariance ET data and processing, and errors and data quality in the user reported pumpage data.

Calibrated METRIC ET estimates likely are accurate within 10 to 20 percent of actual ET on a seasonal time step (Allen and others, 2007). The gridMET reference ET was bias corrected using AgriMet station reference ET data to decrease potential bias, but local differences between gridded reference ET and ground stations likely exist. The uncertainty of the METRIC ET estimate was further reduced by adjusting to measured ET from an eddy covariance station, which has reported accuracies of 10 percent (Meyers and Baldocchi, 2005), assuming the ratio of METRIC ET to station ET was stationary back to 1991. The basin-average seasonal ET and net ET rates from groundwater irrigated fields fall within the range of Harney Basin alfalfa crop ET and net irrigation water requirements (NIWR), respectively, reported in Cuenca and others (1992), which has been used to estimate crop water use across the state of Oregon (ET = 1.57-1.77 ft/yr, NIWR = 1.42-1.71 ft/yr; adjusted to May-September growing season). However, average seasonal rates estimated from surface water irrigated fields, which are predominantly pasture grass, were about 30 percent below median ET and NIWR rates reported by Cuenca and other (1992) for pasture grass (ET = 2.18-2.44 ft/yr, NIWR = 1.87-2.34 ft/yr; adjusted to the May-September growing

season). Lower seasonal rates from surface water irrigated fields, with respect to previous estimates, are not surprising given the limited surface water supply late in the growing season. Growing season net ET from an irrigated field was assumed to represent the lower bound of crop water use because it assumes all precipitation is used for ET (100 percent effective).

Groundwater irrigation efficiency estimates made in this study also fall within the range of literature values for the common irrigation systems (pivot, sprinkler, flood) in the basin. Some unirrigated fields possibly were included in the mapped acreages and basin summaries because of difficulty establishing a minimum threshold for excluding fields based on the remotely-sensed imagery and other datasets, but the effect on the overall ET volumes and acreage was likely small (within 5 percent).

8. REFERENCES

- Abatzoglou, J.T., 2013, Development of gridded surface meteorological data for ecological applications and modelling: *International Journal of Climatology*, v. 33, no. 1, p. 121–131.
- Allen, R.G., Burnett, B., Kramber, W., Huntington, J., Kjaersgaard, J., Kilic, A., Kelly, C., and Trezza, R., 2013, Automated Calibration of the METRIC-Landsat Evapotranspiration Process: *JAWRA Journal of the American Water Resources Association*, v. 49, no. 3, p. 563–576.
- Allen, R.G., Pereira, L.S., Raes, D., and Smith, M., 1998, *Crop Evapotranspiration: Guidelines for Computing Crop Water Requirements*: Food and Agriculture Organization of the United Nations 56, 300 p.
- Allen, R.G., and Tasumi, M., 2005, Evaporation from American Falls Reservoir in Idaho via a Combination of Bowen Ratio and Eddy Covariance, *in World Water and Environmental Resources Congress – ASCE*, Anchorage, Alaska, United States, p. 1–17.
- Allen, R.G., Tasumi, M., Morse, A., Trezza, R., Wright, J.L., Bastiaanssen, W., Kramber, W., Lorite, I., and Robison, C.W., 2007, Satellite-Based Energy Balance for Mapping Evapotranspiration with Internalized Calibration (METRIC)—Applications: *Journal of Irrigation and Drainage Engineering*, v. 133, no. 4, p. 395–406.
- Allen, R.G., Trezza, R., Tasumi, M., and Kjaersgaard, J., 2014, *METRIC: Mapping Evapotranspiration at High Resolution -- Applications Manual for Landsat Imagery (Version 3.0)*: University of Idaho.
- Anderson, M.C., Allen, R.G., Morse, A., and Kustas, W.P., 2012, Use of Landsat thermal imagery in monitoring evapotranspiration and managing water resources: *Remote Sensing of Environment*, v. 122, p. 50–65.
- Arnone, J.I., Jasoni, R., Larsen, J., Fenstermaker, L., Wohlfahrt, G., Kratt, C., Lyles, B., Healey, J., Young, M., and Thomas, J., 2008, Variable evapotranspirative water losses from lowland agricultural and native shrublands ecosystems in the eastern Great Basin of Nevada, USA: *Desert Research Institute DRI Pub. #: 655.7250*.
- Baldocchi, D.D., 2003, Assessing the eddy covariance technique for evaluating carbon dioxide exchange rates of ecosystems: past, present and future: *Global Change Biology*, v. 9, no. 4, p. 479–492.
- Baldocchi, D., Falge, E., Gu, L., Olson, R., Hollinger, D., Running, S., Anthoni, P., Bernhofer, Ch., Davis, K., Evans, R., Fuentes, J., Goldstein, A., Katul, G., Law, B., and others, 2001, FLUXNET: A New Tool to Study the Temporal and Spatial Variability of Ecosystem-Scale Carbon Dioxide, Water Vapor, and Energy Flux Densities: *Bulletin of the American Meteorological Society*, v. 82, no. 11, p. 2415–2434.
- Bredehoeft, J., 2007, It Is the Discharge: *Groundwater*, v. 45, no. 5, p. 523–523.
- Conlon, T.D., Wozniak, K.C., Woodcock, D., Herrera, N.B., Fisher, B.J., Morgan, D.S., Lee, K.K., and Hinkle, S.R., 2005, *Ground-water hydrology of the Willamette basin, Oregon: Scientific Investigations Report 2005–5168*, accessed at <http://pubs.er.usgs.gov/publication/sir20055168>.

- Cooper, R., 2002, Determining surface water availability in Oregon: Oregon Water Resources Department SW 02-002, 157 p., accessed at <https://www.oregon.gov/owrd/wr/docs/sw02-002.pdf>.
- Cosgrove, B.A., Lohmann, D., Mitchell, K.E., Houser, P.R., Wood, E.F., Schaake, J.C., Robock, A., Marshall, C., Sheffield, J., Duan, Q., Luo, L., Higgins, R.W., Pinker, R.T., Tarpley, J.D., and others, 2003, Real-time and retrospective forcing in the North American Land Data Assimilation System (NLDAS) project: *Journal of Geophysical Research: Atmospheres*, v. 108, no. D22.
- Cuenca, R.H., Nuss, J.L., Martinez-Cob, A., and Katul, G.G., 1992, Oregon crop water use and irrigation requirements: Oregon State University 8530.
- Doorenbos, J., and Pruitt, W.O., 1977, Guidelines for predicting crop water requirements: Food and Agriculture Organization of the United Nations FAO Irrigation and Drainage Paper F2430E, 154 p., accessed November 14, 2019, at <http://www.fao.org/publications/card/en/c/6bae3071-5d7b-5206-af5c-c9bfa1d9d1fe/>.
- Foga, S., Scaramuzza, P.L., Guo, S., Zhu, Z., Dilley, R.D., Beckmann, T., Schmidt, G.L., Dwyer, J.L., Joseph Hughes, M., and Laue, B., 2017, Cloud detection algorithm comparison and validation for operational Landsat data products: *Remote Sensing of Environment*, v. 194, p. 379–390.
- Foken, T., 2008, The Energy Balance Closure Problem: An Overview: *Ecological Applications*, v. 18, no. 6, p. 1351–1367.
- Gannett, M.W., Lite Jr., K.E., La Marche, J.L., Fisher, B.J., and Polette, D.J., 2007, Ground-Water Hydrology of the Upper Klamath Basin, Oregon and California: Scientific Investigations Report 2007–5050, accessed at <http://pubs.er.usgs.gov/publication/sir20075050>.
- Gannett, M.W., Lite Jr., K.E., Morgan, D.S., and Collins, C.A., 2001, Ground-Water Hydrology of the Upper Deschutes Basin, Oregon: U.S. Geological Survey Water-Resources Investigations Report 2000–4162, accessed November 15, 2019, at <http://pubs.er.usgs.gov/publication/wri20004162>.
- Garcia, C.A., Corson-Dosch, N.T., Beamer, J.P., Overstreet, B.T., Haynes, J.V., Grondin, G.H., Gingerich, S.B., and Hoskinson, M.D., 2021, Hydrologic Budget of the Harney Basin Aquifer System, Oregon: U. S. Geological Survey Scientific Investigations Report 2021–XXXX.
- Gingerich, S.B., Johnson, H.M., Boschmann, D.E., Grondin, G.H., and Garcia, C.A., 2021, Groundwater Resources of the Harney Basin, Oregon: U. S. Geological Survey Scientific Investigations Report 2021–XXXX.
- Grondin, G.H., 2015, Harney Basin: Permitted Groundwater Rights and Groundwater Budget: Oregon Water Resources Department.
- Huntington, J.L., Hegewisch, K.C., Daudert, B., Morton, C.G., Abatzoglou, J.T., McEvoy, D.J., and Erickson, T., 2017, Climate Engine: Cloud Computing and Visualization of Climate and Remote Sensing Data for Advanced Natural Resource Monitoring and Process Understanding: *Bulletin of the American Meteorological Society*, v. 98, no. 11, p. 2397–2410.

- Huntington, J. L., Gangopadhyay, S., Spears, J.M., Allen, R.G., King, C., Morton, C.G., Harrison, A., McEvoy, D., Joros, A., and Pruitt, T., 2015, West-wide climate risk assessments: Irrigation demand and reservoir evaporation projections: U.S. Bureau of Reclamation, US Department of the Interior, Bureau of Reclamation, Technical Service Center 86-68210-2014-01, 196 p.
- Meyers, T.P., and Baldocchi, D.D., 2005, Current Micrometeorological Flux Methodologies with Applications in Agriculture, *in* Micrometeorology in Agricultural Systems: John Wiley & Sons, Ltd, p. 381–396.
- Morton, C.G., Huntington, J.L., Pohl, G.M., Allen, R.G., McGwire, K.C., and Bassett, S.D., 2013, Assessing Calibration Uncertainty and Automation for Estimating Evapotranspiration from Agricultural Areas Using METRIC: JAWRA Journal of the American Water Resources Association, v. 49, no. 3, p. 549–562.
- Pastorello, G., Trotta, C., Canfora, E., Chu, H., Christianson, D., Cheah, Y.-W., Poindexter, C., Chen, J., Elbashandy, A., Humphrey, M., Isaac, P., Polidori, D., Reichstein, M., Ribeca, A., and others, 2020, The FLUXNET2015 dataset and the ONEFlux processing pipeline for eddy covariance data: Scientific Data, v. 7, no. 1, p. 225.
- Robison, J.H., 1968, Estimated Existing and Potential Ground-water Storage in Major Drainage Basins in Oregon: U.S. Geological Survey.
- Sarwar, A., Peters, R.T., Mehanna, H., Amini, M.Z., and Mohamed, A.Z., 2019, Evaluating water application efficiency of low and mid elevation spray application under changing weather conditions: Agricultural Water Management, v. 221, p. 84–91.
- State of Nevada Division of Water Resources, 2017, Statewide Groundwater Pumpage Inventory, Calendar Year 2015: Department of Conservation and Natural Resources, Division of Water Resources, 29 p., accessed at http://water.nv.gov/documents/Nevada_Groundwater_Pumpage_2015.pdf.
- State of Oregon Water Resources Board, 1967, Malheur Lake Basin: Oregon Water Resources Department OWRD Basin Report.
- Tasumi, M., Allen, R.G., Trezza, R., and Wright, J.L., 2005, Satellite-Based Energy Balance to Assess Within-Population Variance of Crop Coefficient Curves: Journal of Irrigation and Drainage Engineering, v. 131, no. 1, p. 94–109.
- Twine, T.E., Kustas, W.P., Norman, J.M., Cook, D.R., Houser, P.R., Meyers, T.P., Prueger, J.H., Starks, P.J., and Wesely, M.L., 2000, Correcting eddy-covariance flux underestimates over a grassland: Agricultural and Forest Meteorology, v. 103, no. 3, p. 279–300.
- University of Edinburgh, 2013, EdiRe Software for Micrometeorological Applications: University of Edinburgh, UK.
- USDA, 2008, U.S. Department of Agriculture Common Land Unit dataset:
- USDA, 2016, U.S. Department of Agriculture National Agriculture Imagery Program dataset:

USDA National Agricultural Statistics Service, 2018, 2018 Oregon Annual Statistical Bulletin: U. S. Department of Agriculture.

Volk, J., Huntington, J., Allen, R., Melton, F., Anderson, M., and Kilic, A., review pending, flux-data-qaqc: A Python Package for Energy Balance Closure and Post-Processing of Eddy Flux Data: Journal of Open Source Software, v. 6, p. 1–5.

Washington State Department of Ecology, 2005, Determining Irrigation Efficiency and Consumptive Use: Washington State Department of Ecology GUID-1210.

Wohlfahrt, G., Fenstermaker, L.F., and Iii, J. a. A., 2008, Large annual net ecosystem CO₂ uptake of a Mojave Desert ecosystem: Global Change Biology, v. 14, no. 7, p. 1475–1487.

Zhao, W., R.G. Allen, R. Trezza, and C.W. Robison, 2014, Production of Satellite-based Maps of Evapotranspiration using the METRIC Model for Year 2010 for Landsat Path 43 Row 29 the Powder River Basin of Oregon: University of Idaho.

Zhao, W., R.G. Allen, R. Trezza, and C.W. Robison, 2015, Production of Satellite-based Maps of Evapotranspiration using the METRIC Model for Year 2013 in the Klamath River Basin of Oregon - Landsat Path 45 Rows 30 and 31: University of Idaho, 113 p., accessed at <https://app.box.com/s/9g3s4hj7p8r1ij3h340777olskzfpo8m>.

APPENDIX A. GLOSSARY OF TERMS

AgriMET – A network of agricultural weather stations operated by the U.S. Bureau of Reclamation.

Bowen ratio – The Bowen ratio method for flux measurement is derived from the energy balance of the underlying surface. It is the ratio of heat flux to moisture flux near the surface.

Common Land Unit (CLU) - the smallest unit of land that has a permanent, contiguous boundary, a common land cover and land management, a common owner and a common producer in agricultural land associated with USDA farm programs. Vector polygon (shapefile) dataset.

Consumptive Use (CU) - The part of water withdrawn that is evaporated, transpired, incorporated into crops, or otherwise consumed from immediate water environment.

Cropland Data Layer (CDL) – Raster, georeferenced, crop-specific land cover data layer created annual for the continental United States using moderate resolution satellite imagery and extensive agricultural ground truth.

Eddy Covariance (EC) – A micro-meteorological method that is currently popular to directly observe the exchanges of gas, energy, and momentum between ecosystems and the atmosphere.

Evapotranspiration (ET) - The combined processes by which water is transferred from the earth's surface to the atmosphere; evaporation of liquid or solid water plus transpiration from plants.

ET_o – (Reference ET) refers to the ET equations calibrated to estimate the water use of a well-watered grass field under a set of local weather conditions computed using the ASCE standardized Penman-Montieth equation.

ET_r – (Reference ET) refers to the ET equations calibrated to estimate the water use of a well-watered alfalfa field under a set of local weather conditions computed using the ASCE standardized Penman-Montieth equation.

ET_rF – Fraction of reference ET computed as actual ET divided by reference ET. Synonymous with the crop coefficient (K_c).

FGDC (Federal Geographic Data Committee) – The FGDC develops or adopts geospatial standards. Federal agencies that collect, use, or disseminate geographic information and/or carry out related spatial data activities are required to use FGDC-endorsed standards. Non-Federal agencies are encouraged to use FGDC-endorsed standards to facilitate data sharing.

gridMET - A gridded dataset of daily high-spatial resolution (~4-km, 1/24th degree) surface meteorological data covering the contiguous US from 1979-yesterday.

K_c - Ratio of ET occurring with specific crop at specific stage of growth to reference ET.

Irrigation efficiency – The ratio of the volume of water required for a specific beneficial use as compared with the volume of water delivered for this purpose. It is commonly interpreted as the volume of water stored in the soil for evapotranspiration compared with the volume of water delivered for this purpose.

METRIC – Mapping Evapotranspiration using high Resolution and Internalized Calibration model. METRIC calculates ET as a residual of the surface energy balance using satellite imagery calibrated to in-situ reference ET from weather stations or a gridded product.

Net ET – Total ET less precipitation. (As opposed to Total ET.)

Net Irrigation Water Requirement (NIWR) - The quantity of water exclusive of precipitation that is required for various beneficial uses, particularly evapotranspiration.

Normalized Difference Vegetation Index (NDVI) - A common and widely used remote sensing index that is computed as the difference between near-infrared (NIR) and red (RED) reflectance divided by their sum.

Place of Use (POU) – OWRD-developed GIS vector (polygon) file that shows the locations of where water rights are used or applied

Potential evapotranspiration – the rate at which water if available would be removed from wet soil and plant surfaces expressed as the rate of latent heat transfer per unit area or an equivalent depth of water.

Raster – Dataset consisting of a matrix of cells (or pixels) organized into rows and columns (or a grid) where each cell contains a value representing information.

Reference ET - ET equations calibrated to produce ET for a defined reference crop (generally clipped, cool season grass or full cover alfalfa) under a set of local weather conditions. In this study reference ET computed using the ASCE standardized Penman-Monteith equation.

SSURGO - The Soil Survey Geographic database contains information about soil as collected by the National Cooperative Soil Survey over the course of a century.

Total ET – measurement of evapotranspiration from a combination of irrigation sources plus precipitation. (As opposed to Net ET.)

Water Year – Twelve -month period from October 1 for a given year through September 30, of the following year. The water year is designated by the calendar year in which it ends.